FACULTY OF SCIENCE AND TECHNOLOGY

BACHELOR'S THESIS

Study programme / specialisation: Biological Chemistry	The spring semester, 2023 Open
Author: Cecilie Meidell Knutsen	
Supervisor at UiS: Malcolm Andrew Kelland	
Thesis title: Crystal Growth Inhibition of Tetrahydrofuran Hydrates with Ring-Structured Amine Oxides	
Credits (ECTS): 20	
Keywords: Tetrahydrofuran (THF) Hydrate Hydrate Inhibition Heterocyclic Amine Oxides Cycloalkyl Amine Oxides Branched vs. Linear Polymers	Pages: 67 + appendix: 9 Stavanger, 05.06.2023

Approved by the Dean 30 Sep 21
Faculty of Science and Technology

BACHELOR´S THESIS

Crystal Growth Inhibition of Tetrahydrofuran Hydrates with Ring-Structured Amine Oxides

By Cecilie Meidell Knutsen

Spring 2023

Abstract

Gas hydrates are clathrate crystalline solids created when water and small gas molecules are subjected to high pressures and low temperatures. Gas hydrate formation is a major problem in the oil and gas industry as it can plug subsea pipelines and stop production. Many methods are used to prevent gas hydrate formation, including chemical treatments. Thermodynamic hydrate inhibitors (THIs) and low-dosage hydrate inhibitors (LDHIs) are different chemical treatments used commercially today. LDHIs have two subclasses: kinetic hydrate inhibitors (KHIs) and anti-agglomerants (AAs).

This thesis's first project aimed to synthesize and test a series of amine oxides with ring structures, either cycloalkyl or heterocyclic groups, to see if they had the potential to be KHI synergists or AAs in the oil and gas industry. The test method used is called the THF-hydrate crystal growth test, where the crystal growth is measured in grams/ hour. The cycloalkyl amine oxides showed excellent inhibiting performance of THF hydrates. Especially the amine oxides with 6- and 7-membered cycloalkyl groups alkylated with butyl and pentyl. They inhibited THF hydrates at certain concentrations better than TBAB, TPAB, TBAO, and TPAO and should be further tested on gas hydrate mixtures as potential KHI synergists or AAs. Different placements and numbers of the cycloalkyl groups on amine oxides were carried out to find the best cycloalkyl amine oxide inhibitor. It was confirmed that one cycloalkyl group bonded to an amine oxide increased the inhibiting performance as an alkylamine was butylated to compare. The different heterocyclic amine oxides (4000 ppm) gave poor inhibiting performances of THF hydrate. One exception was Di-n-butyltetrahydrofurfurylamine oxide which gave a better inhibition performance than the commercially used TBAB.

The thesis's second project entailed comparing the inhibition of THF hydrates of the commercially used linear polymer Polyvinylcaprolactam (PVCap) with different branched polymers. This was evaluated by comparing the limiting concentration for zero growth (LCZG) on a THF rig. Unreliable results caused by the low water solubility of the branched polymers impacted the project´s success. Yet, the branched polymer trimethylolpropane triacrylate (60:1) with three branches showed a better LCZG (2100 ppm) than PVCap (3000 ppm).

Acknowledgments

I would like to express my gratitude to my supervisor Professor Malcolm Andrew Kelland, for giving me the opportunity to work with him on this thesis and for his guidance, advice, and professional support during this semester.

I would also like to thank Ali Hasan Saber Alkaraly, Hiwot Minwuyelet Tiruye, and Venkatesh Bollabathini for running ^{1}H-NMR analyses on all of my samples.

I would also like to thank Janronel Calog Pomicpic for helping me in the laboratory and Erik Gisle Dirdal for letting me use his branched polymers for a part of my project.

Finally, I would like to thank my family and friends for always supporting me.

Table of Contents

Chapter 1. Introduction

The overview of the fundamentals of gas hydrate, issues related to gas hydrate formation in the oil and gas industry, and preventive measures for these issues will be covered in this chapter to better understand the thesis's objective.

1.1 Fundamentals of Gas Hydrate

Gas hydrates are clathrate solids that resemble ice and are created when water and gas are subjected to high pressures and low temperatures.[1, 2] The water molecules form an open three-dimensional structure, often called a cage, bound together with hydrogen bonds. The cages contain various gas molecules such as hydrocarbons (methane, ethane, propane, and isobutane) and some non-hydrocarbons like hydrogen sulfide, carbon dioxide, and nitrogen. The type of gas molecule that is present depends on the structure of the cage.[3] They stabilize the structure by van der Waals interactions, and when a molecule behaves this way, it is categorized as a clathrate. There are three possible gas hydrate structures formed, as seen in Figure 1.1: structure I (sI), structure II (sII), and structure H (sH). However, sH is rarely found in the oil industry.[4]

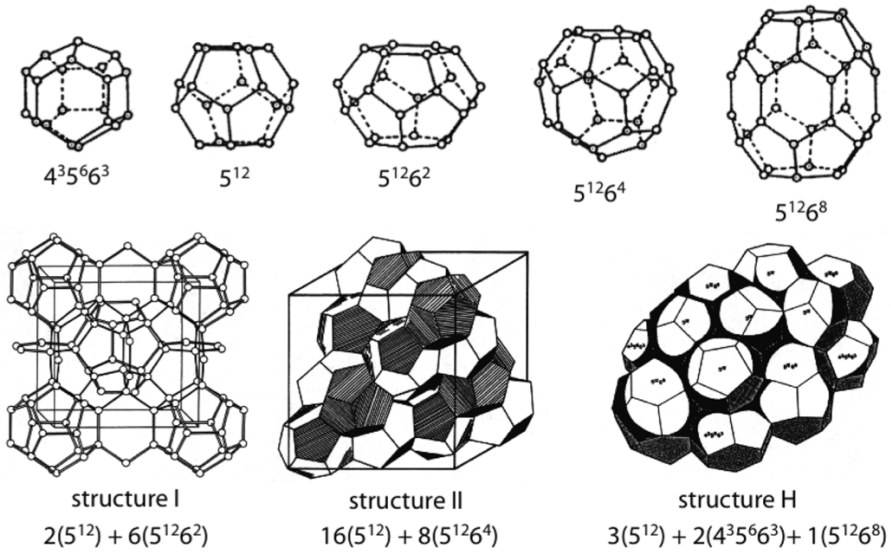

Figure 1.1 Gas hydrate crystal structures formed by water cages.[3]

The formation of gas hydrates only happens when the right conditions occur. The combination of temperature and pressure must be right, where low temperatures and high pressures are optimal for stability. The presence of a gas molecule, e.g., methane, ethane, carbon dioxide, etc., and sufficient amounts of water are also needed for the formation. These three criteria are interconnected, meaning removing one prevents hydrate formation altogether.[5] Figure 1.2 shows a pressure-temperature graph for a typical natural gas hydrate. Gas hydrates can form at temperatures as high as 25-30 °C under high-pressure conditions.

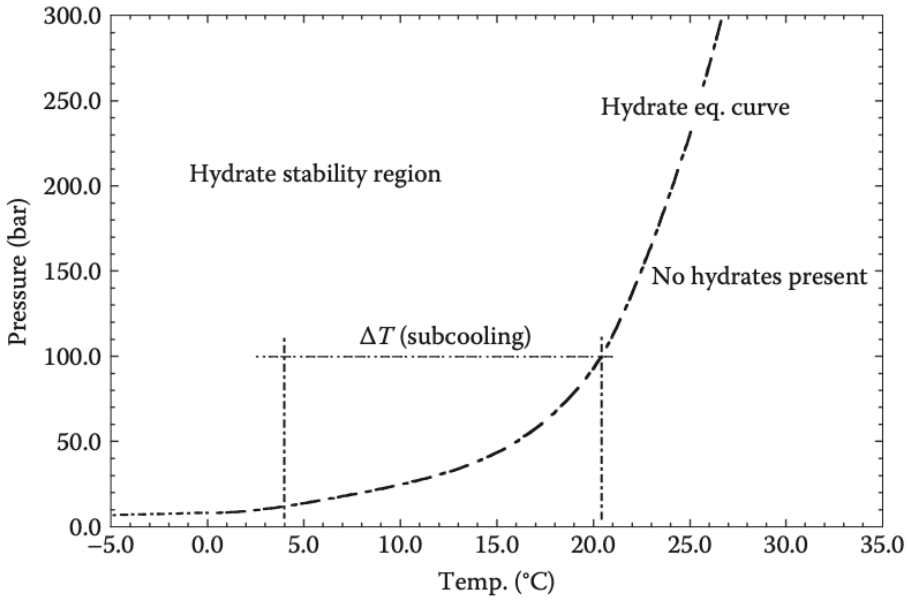

Figure 1.2 An example of a pressure–temperature graph for a typical natural gas hydrate.[4]

1.2 Gas Hydrate in the Oil Industry

The oil and gas industry encounters challenging conditions with offshore explorations of hydrocarbons in deep and cold waters. For hydrocarbon transport, the production facilities require long subsea tiebacks from the wellhead to the production platforms and subsea pipelines to transport refined gas and condensation steam to export facilities.[6] High pressures and low temperatures are standard in deep water oil and gas fields, and as mentioned earlier, these conditions are optimal for hydrate formation. The multiphase fluid (water-oil-gas) produced at the wellhead usually cools as it travels through the subsea pipes, which means that hydrate formation is likely to occur. Additionally, hydrate formation can happen under shut-ins and startups as the pipeline temperatures fall to the temperature of the ocean floor.[7]

Gas hydrate formation is considered one of the biggest challenges regarding flow assurance in the pipelines subsea. Gas hydrate structures I and II are known to be formed in these pipelines. Structure I is formed from natural gas high in methane, and structure II is formed from a mixture of natural gases.[8] Gas hydrates pose a serious operational problem because the hydrate crystals form on the pipeline walls and eventually build up as large plugs (see Figure 1.3), blocking pipelines and resulting in overpressures that eventually force the production facilities to shut down. Even though gas hydrates have the potential to source hydrocarbon energy and be a method of sorting and transmitting natural gases, these plugs can accelerate by pressure which can pose a severe safety and environmental risk, as well as damage the production facilities. In addition to posing safety risks, removing hydrate plugs from subsea production can be time-consuming and expensive. To ensure that the pipelines operate normally, it is necessary to use methods that efficiently avoid the formation of gas hydrates in the pipelines subsea.[7]

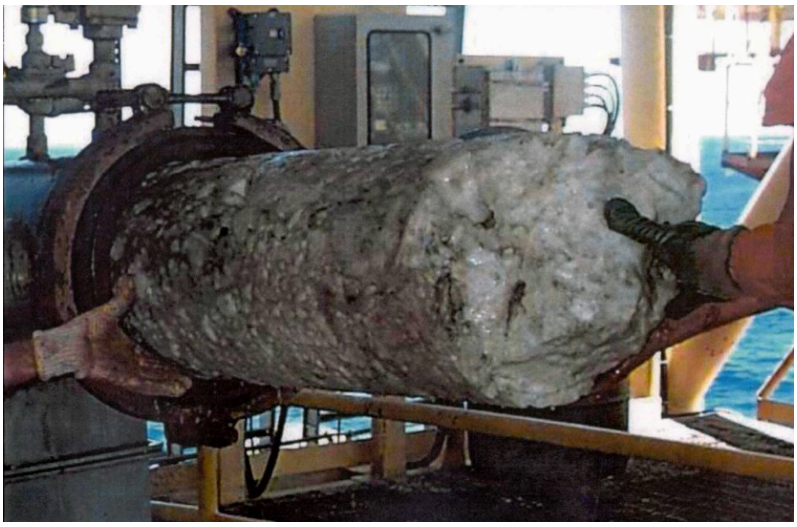

Figure 1.3 Gas hydrate plug removal from a flow line.[8]

1.3 Methods for Preventing Gas Hydrate Formation

There has been developed a few methods for preventing gas hydrate formation, and some of them are: [7]

- Maintaining low pressure outside the area where hydrates are stable.
- Maintaining a temperature higher than the hydrate-stable zone using active heating or passive heat retention.
- Water separation (dehydration).
- Adding another gas to the gas phase to modify it.
- Chemical-free conversion of water into portable hydrate particles.
- Chemical treatment.

Maintaining low pressures can be performed during shut-in, but keeping the pressure low continuously is uncommon because the production rates would be too low to be profitable.[9] Another drawback of this approach is that when dealing with deep water, the fluids in the hydrate-stable zone are kept in place by the hydrostatic pressure of the water. A pipeline´s temperature can be increased in a number of ways to prevent the formation of gas hydrates. Insulating the pipes is the simplest method. Thermal insulating fluids[10] is an insulation method that has been increasingly used. Burying the pipelines, wrapping them in insulation materials, or creating a vacuum around them are other methods, but the latter is costly and would not work during prolonged shutdowns. Direct electric heating of a pipeline employing an alternating current is a different method utilized on several North Sea fields.[11] This method is only used during prolonged shutdowns since it is too expensive to use continuously. Water separation from oil and gas is a critical method to prevent the formation of hydrates. Many long-distant transportation lines have used it. However, it can be difficult or costly, especially in the production pipelines.[12] Injecting a gas like nitrogen (N_2) or carbon dioxide (CO_2) is another approach that initially looks counterintuitive in order to increase the pressure threshold for hydrate formation.[13] Conversion of water into portable hydrate particles without using chemicals is a method called “cold-flow”.[14] The hydrate particles will remove free water from the remainder of the transport system since they are dry, nondepositing, and nonagglomerating. There are also different chemical treatment methods used for preventing gas hydrate formation, these will be discussed next.

1.4 Chemical Inhibition of Gas Hydrates

Chemical inhibition to prevent hydrate formation can be separated into three groups: thermodynamic hydrate inhibitors (THIs), kinetic hydrate inhibitors (KHIs), and anti-agglomerants (AAs). Collectively, KHIs and AAs are known as low-dosage hydrate inhibitors (LDHIs).

1.4.1 Thermodynamic Hydrate Inhibitors (THIs)

Thermodynamic hydrate inhibitors are the most commonly used chemical inhibition group to prevent hydrate formation. They work by shifting the pressure-temperature equilibrium to a lower temperature and a higher pressure. The most frequently used THIs are alcohols, glycols, and salts. However, these conventional hydrate inhibitors must be injected up to 100% of the water weight (100 wt.%) to be effective.[15]

Monoethylene glycol (MEG, HOCH2CH2OH) and methanol (CH3OH) are often used to prevent the formation of hydrates during production, workover, and process activities, as well as to melt hydrate plugs. Although they are less effective, diethylene glycol (DEG) and triethylene glycol (TEG) are also occasionally used to stop the formation of hydrates. The major application of TEG is gas drying, which is water adsorption in gas flowlines or processing facilities.[4] Because methanol and glycols are dosed at high concentrations, even though they are relatively inexpensive chemicals, it is economically beneficial to recover the THI and use it again. Methanol regeneration is substantially less common than MEG regeneration.[16] Due to the large amounts of water that must be processed, methanol and glycols are rarely used continuously in oil fields. However, MEG is frequently used continuously in condensate and gas fields.[17] Correct THI dosage is crucial as using a dosage that only partially protects against hydrate formation will enhance the clogging potential.[18]

THIs has several operational problems due to the high amount of chemicals needed to be effective. This includes large storage tanks, costly transportation, and injection lines. The development of LDHIs in the 1990s was a result of this.

1.4.2 Kinetic Hydrate Inhibitors (KHIs)

As mentioned before, kinetic hydrate inhibitors (KHIs) are low-dosage hydrate inhibitors (LDHIs). Compared to THIs, they can be administered in small volumes (<1 wt.%) without interfering with pipeline flow and not requiring additional separation devices to separate them from the fluid. [3] Gas hydrate nucleation and crystal growth are both delayed by KHIs for a duration that is affected by the subcooling and, to some extent, the system pressure. The most significant disadvantage of KHIs is that they stop working when the subcooling temperature exceeds 12 °C. [15] Greater subcooling would result in shorter hydrate formation delay times, and in most deep-water fields where subcooling and pressure are high, KHIs are not applicable.[19]

It has been demonstrated that several water-soluble polymers act as KHIs, often containing small organic molecules, that enhance the effect of the KHIs. They are called synergists. Many synergists exist, but specific solvents and quaternary ammonium ("quat") salts are widely used.[1] Quats are discussed more in the next subchapter, 1.4.3. A KHI polymer has two essential structural characteristics. The polymer first requires functional groups that can form hydrogen bonds with water molecules or the surfaces of gas hydrate particles to inhibit the hydrate formation. Typically, these are amide groups. The second distinguishing characteristic is a hydrophobic group next to or chemically attached to each amide group. This group can act as the quest molecule that resides in the cage formation of the gas hydrate and can inhibit further growth. [20]

Polyvinylpyrrolidone (PVP) was the first KHI discovered. Without any synergists, the subcooling for PVP at 70-90 bar is only 3-4 °C. Due to its poor performance, vinylcaprolactam polymers (VCap), with about 9-10 °C subcooling under the same conditions, replaced them. [21–25] Other commercially used polymers are polyvinylcaprolactam (PVCap), the copolymer vinylpyrrolidone/vinylcaprolactam (VP/VCap), other VCap copolymers, polymers of N-isopropylmethacrylamide and hyperbranched polyesteramides.[4] Figure 1.4 shows the structure of the different polyvinyllactam polymers.

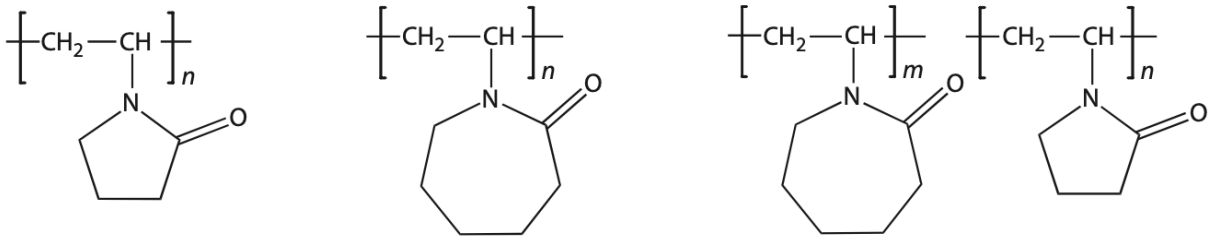

Figure 1.4 Poly-N-vinyllactam polymers: Polyvinylpyrrolidone (PVP), polyvinylcaprolactam (PVCap), and vinylpyrrolidone/vinylcaprolactam copolymer (VP/VCap). [4]

One part of the project was determining whether branched polymers inhibited tetrahydrofuran (THF) hydrate crystal growth more than the commercially used linear polymers. More on this subject will be discussed in Chapter 4.

1.4.3 Anti-agglomerants (AAs)

Anti-agglomerants (AAs) are the other low-dosage hydrate inhibitor group. AAs are efficient at high subcooling, in contrast to KHIs. AAs may not slow down the growth of the hydrate. Still, they can stop small hydrate particles from coalescing into larger hydrate pieces and delays the pipeline blockage until the pipeline reaches higher temperatures and lower pressure conditions. They contain surfactant-like chemical groups, like molecules with hydrophilic and oleophilic functions, making them interact with water and oil in the pipelines.[26] AAs are categorized into two subclasses: production or pipeline AAs and gas-well AAs. The formation of hydrates as a transportable slurry of hydrate particles in the hydrocarbon liquid phase is made possible by pipeline AAs. Gas-well AAs spread the hydrate particles in excess water.[4] Figure 1.5 shows quaternary ammonium surfactants with two and three n-butyl groups.

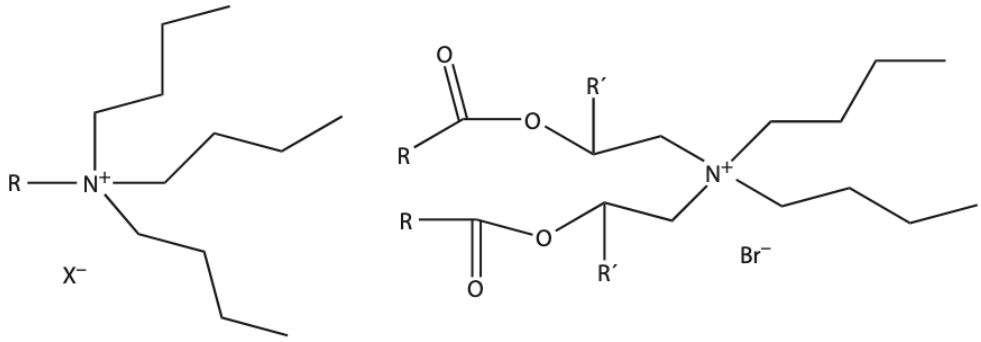

Figure 1.5 General structures of single- and twin-tailed butylated quaternary ammonium AAs. R = long alkyl chain. R´= H or CH_3, X = counterion.[4]

The most well-known AAs are quaternary ammonium ("quat") surfactants, which Shell created and patented in the early 1990s from studies on inhibiting THF hydrate crystal growth. Tetrabutylammonium bromide (TBAB) and Tetrapentylammonium bromide (TPAB) are examples of quats they patented.[27] Quaternary surfactants consist of an ammonium or phosphonium salt as the hydrate-philic headgroup with two or more hydrophobic groups, where n-butyl, n-pentyl, or iso-pentyl are the most common. They work by accumulating where the hydrate formation first occurs, in the water-oil interface. The hydrate-philic headgroup will attach to hydrate particles and the butyl/pentyl groups will penetrate open cavities on the hydrate surface. When the quats have a long hydrophobic tail, it prevents the hydrate from expanding on that surface.[1] When the quaternary salts are used as KHI synergists, it is thought that the geometry difference between the PVCap and the quat is the reason why it works. They should attach to different sites on the hydrate surface and therefore enhance the effect of the KHI.[28]

Research on amine oxides as a different class of nonionic surfactant AAs was conducted about 25 years ago. A more thorough study on a wide range of amine oxides was reported 10 years ago. This included tests of THF hydrate crystal growth with trialkyl amine oxides. The best THF crystal growth inhibitors (CGIs) were found to be tri-n-butylamine oxide (TBAO), tri-n-pentylamine oxide (TPAO), and tri-iso-pentylamine oxide (TiPAO).[29] Trialkyl amine oxides have a structure that is similar to quats, as seen in Figure 1.6. They both have an ammonium ion as the hydrate-philic head group, with four groups attached. The difference is that the quat has four attached hydrophobic alkyl groups, while the amine oxide has three alkyl groups and a nitrogen-oxygen bond.

Figure 1.6 General structures of tertiary amine oxide (left) and quaternary -onium surfactant (right), M = N or P, X = counterion, R = alkyl group

Amine oxides and quats bond to the hydrate surfaces differently. Since amine oxides have a negatively charged oxygen, they will bond to the hydrate surface with hydrogen bonding. Quats do not have the amine oxide group and only bond with van der Waals interactions, which is a much weaker bond.[29] Based on the knowledge that amine oxides work excellent as THF CGIs, the other part of the project was to see if amine oxides with ring structures, either cycloalkyl or heterocyclic groups, would inhibit THF hydrate crystal growth and have the potential to be used as both AAs, and KHI synergists in the oil and gas industry. The ring structure attached to the amine oxides may mimic the alkane gas molecules that fit inside the cages of the gas hydrates by van der Waals interactions. Ring amine oxides have previously been investigated before with polyether cycloimine oxide rings which displayed a good inhibiting performance [30], but small cyclic amine oxides have not yet been investigated.

1.4.4 Testing of Low-dosage Hydrate Inhibitors (LDHI)

Before a chemical can be used in oil fields, numerous tests on the performance of the chemical need to be carried out. This is to better understand how the chemical's inhibition will be in different conditions and how it potentially will affect the environment.

1.4.4.1 Performance Testing of KHIs

The performance of KHIs can be evaluated using a variety of methods. The minimum hold time (the time between when the system reaches the hydrate stability region and when hydrate formation starts) in worst-case subcooling conditions is determined if an operator is interested in qualifying a chemical for field use.[31, 32] Since the flowline is not always at the maximum subcooling and pressure, this will provide a conservative estimate of the dosage needed to

eliminate hydrate issues. The tests should also be conducted at system pressure because, according to numerous studies, hold times change with pressure even when subcooling is present.[33–35] For field verification under planned or unforeseen shut-in conditions, shut-in tests without flow must be included. Testing with additional production chemicals is also important to verify if they affect the inhibitor. Autoclaves, rocking cells, pipe wheels, or loops are all test equipment in which the tests can be carried out with the fluid and gas composition of the actual field.[4]

KHIs (and crystal growth-modifying AAs) can be evaluated using induction time and CGI experiments on THF hydrate at atmospheric pressure. The latter will be discussed in more detail in Chapter 2. Some KHIs may not perform as well with this method as THF is highly water soluble, and the inhibition mechanism may not be the same as in a real gas system.[36]

1.4.4.2 Performance Testing of AAs

The performance testing of AAs in laboratories includes rocking cells, autoclaves, pipe wheels, and loops with hydrate-forming fluids and the right gas conditions. Rocking cells are a useful equipment for screening AAs under various test conditions and are frequently used by service companies as the initial step in product qualifications. [37] The rocking cells have an observation window (e.g., made of sapphire) and are filled with hydrate-forming fluids. A metal ball is then rocked back and forth. Sensors at the cell´s ends pick up when hydrate formations prevent the ball from reaching the ends.

Normally, it is necessary to evaluate an AAs performance in three different water-cut conditions: [4]

1. Cooling down to the hydrate stable region under flowing conditions.

2. Restart with a prepared hydrate slurry following a shut-in period.

3. Cooling down to the hydrate stable region during a shut-in, then starting back up.

1.5 References

(1) Kelland, M. A. History of the Development of Low Dosage Hydrate Inhibitors. *Energy Fuels* **2006**, *20* (3), 825–847. https://doi.org/10.1021/ef050427x.

(2) Sloan, E. D. Fundamental Principles and Applications of Natural Gas Hydrates. *Nature* **2003**, *426* (6964), 353–363. https://doi.org/10.1038/nature02135.

(3) Sum, A. K.; Koh, C. A.; Sloan, E. D. Clathrate Hydrates: From Laboratory Science to Engineering Practice. *Ind. Eng. Chem. Res.* **2009**, *48* (16), 7457–7465. https://doi.org/10.1021/ie900679m.

(4) Kelland, M. A. *Production Chemicals for the Oil and Gas Industry*, 2nd ed.; CRC Press, 2014.

(5) Carroll, J. *Natural Gas Hydrates: A Guide for Engineers*, 4th ed.; Elsevier Science & Technology, 2020.

(6) Zerpa, L. E.; Salager, J.-L.; Koh, C. A.; Sloan, E. D.; Sum, A. K. Surface Chemistry and Gas Hydrates in Flow Assurance. *Ind. Eng. Chem. Res.* **2011**, *50* (1), 188–197. https://doi.org/10.1021/ie100873k.

(7) Mokhatab, S.; Wilkens, R. J.; Leontaritis, K. J. A Review of Strategies for Solving Gas-Hydrate Problems in Subsea Pipelines. *Energy Sources Part Recovery Util. Environ. Eff.* **2007**, *29* (1), 39–45. https://doi.org/10.1080/009083190933988.

(8) Kelland, M. A. Challenges with Gas Hydrate Formation. *IOP Conf. Ser. Mater. Sci. Eng.* **2019**, *700* (1), 012057. https://doi.org/10.1088/1757-899X/700/1/012057.

(9) R. F. Stoisits, D. C. Lucas, L. D. Talley, D. P. Shatto, and J. Cai. International Patent Application WO/2009/042319.

(10) X. Wang, Q. Qu, P. Joavora, and R. Pearcy. New Trend in Oilfield Flow-Assurance Management: A Review of Thermal Insulating Fluids," SPE 103829. *SPE Prod. Facil.* **2009**, *24* (1), 35–42.

(11) R. R. Roth. "Direct Electrical Heating of Flowlines—A Guide to Uses and Benefits," OTC 22631, OTC Brasil, Rio de Janeiro, Brazil. **2011**.

(12) Almashwali, A. A.; Bavoh, C. B.; Lal, B.; Khor, S. F.; Jin, Q. C.; Zaini, D. Gas Hydrate in Oil-Dominant Systems: A Review. *ACS Omega* **2022**, *7* (31), 27021–27037. https://doi.org/10.1021/acsomega.2c02278.

(13) K. J. Kinnari, C. Labes-Carrier, K. Lunde, and L. Aaberge. International Patent Application WO/2006/027609.

(14) J. W. Lachance, and D. J. Turner. International Patent Application WO/2011/109118.

(15) Zhao, H.; Sun, M.; Firoozabadi, A. Anti-Agglomeration of Natural Gas Hydrates in Liquid Condensate and Crude Oil at Constant Pressure Conditions. *Fuel* **2016**, *180*, 187–193. https://doi.org/10.1016/j.fuel.2016.03.029.
(16) B. Kaasa, and P. H. Billington,. International Patent Application WO/2010/084323.
(17) U. C. Klomp, and A. P. Mehta. "An Industry Perspective on the State-of-the Art of Hydrates Management," Proceedings of the 5th International Conference on Gas Hydrates, Trondheim, Norway,. **2006**.
(18) M. H. Yousif. "Effect of Underinhibition with Methanol and Ethylene Glycol on the Hydrate-Control Process," SPE 50972,. *SPE Prod. Facil.* **1998**, *13(3)*, 184.
(19) Nazeri, M.; Tohidi, B.; Chapoy, A. An Evaluation of Risk of Hydrate Formation at the Top of a Pipeline. *Oil Gas Facil.* **2014**, *3* (02), 67–72. https://doi.org/10.2118/160404-PA.
(20) Varma-Nair, M.; Costello, C. A.; Colle, K. S.; King, H. E. Thermal Analysis of Polymer–Water Interactions and Their Relation to Gas Hydrate Inhibition. *J. Appl. Polym. Sci.* **2007**, *103* (4), 2642–2653. https://doi.org/10.1002/app.25414.
(21) E. D. Sloan. U.S. Patent 5432292. **1995**.
(22) S. B. Fu, L. M. Cenegy, and C. Neff. "A Summary of Successful Field Applications of A Kinetic Hydrate Inhibitor," SPE 65022 (Paper Presented at the SPE International Symposium on Oilfield Chemistry, Houston, TX, February 13–16, 2001).
(23) E. D. Sloan, R. L. Christiansen, J. Lederhos, V. Panchalingam, Y. Du, A. K. W. Sum, and J. Ping. U.S. Patent 5639925. **1997**.
(24) C. B. Argo, R. A. Blaine, C. G. Osborne, and I. C. Priestly. "Commercial Deployment of Low Dosage Hydrate Inhibitors in a Southern North Sea 69 Kilometer Wet-Gas Subsea Pipeline," SPE 37255 (Paper Presented at the SPE International Symposium on Oilfield Chemistry, Houston, TX, February 1997).
(25) L. D. Talley, and G. F. Mitchell. "Application of Kinetic Hydrate Inhibitor in Black-Oil Flowlines," SPE 56770 (Paper Presented at the SPE Annual Technical Conference and Exhibition, September 1999).
(26) Brown, E. P.; Turner, D.; Grasso, G.; Koh, C. A. Effect of Wax/Anti-Agglomerant Interactions on Hydrate Depositing Systems. *Fuel* **2020**, *264*, 116573. https://doi.org/10.1016/j.fuel.2019.116573.
(27) U. C. Klomp, V. C. Kruka, and R. Reijnhart. WO Patent Application 95/17579. **1995**.
(28) Chua, P. C.; Kelland, M. A. Tetra(Iso-Hexyl)Ammonium Bromide—The Most Powerful Quaternary Ammonium-Based Tetrahydrofuran Crystal Growth Inhibitor and Synergist with Polyvinylcaprolactam Kinetic Gas Hydrate Inhibitor. *Energy Fuels* **2012**, *26* (2), 1160–1168.

https://doi.org/10.1021/ef201849t.
(29) Kelland, M. A.; Kvæstad, A. H.; Astad, E. L. Tetrahydrofuran Hydrate Crystal Growth Inhibition by Trialkylamine Oxides and Synergism with the Gas Kinetic Hydrate Inhibitor Poly(N-Vinyl Caprolactam). *Energy Fuels* **2012**, *26* (7), 4454–4464. https://doi.org/10.1021/ef300624s.
(30) Zhang, Q.; Limmer, L.; Frey, H.; Kelland, M. A. *N* -Oxide Polyethers as Kinetic Hydrate Inhibitors: Side Chain Ring Size Makes the Difference. *Energy Fuels* **2021**, *35* (5), 4067–4074. https://doi.org/10.1021/acs.energyfuels.0c04333.
(31) U. C. Klomp, and A. P. Mehta. "Validation of Kinetic Inhibitors for Sour Gas Fields," IPTC-11374 (Paper Presented at the International Petroleum Technology Conference, Dubai, UAE, December 4–6, 2007).
(32) U. Klomp. "The World of LDHI: From Conception to Development to Implementation," Proceedings of the 6th International Conference on Gas Hydrates Vancouver, British Columbia, Canada,. **2008**.
(33) M. Arjmandi, B. Tohidi, A. Danesh, and A. C. Todd. "Is Subcooling the Right Driving Force for Testing Low-Dosage Hydrate Inhibitors?,." *Chem. Eng. Sci.* **2005**, *60*, 1313–1321.
(34) J.-P. Peytavy, P. Glénat, and P. Bourg. "Kinetic Hydrate Inhibitors—Sensitivity towards Pressure and Corrosion Inhibitors," IPTC 11233 (Paper Presented at the International Petroleum Technology Conference, Dubai, UAE, 4–6 December 2007).
(35) M. A. Kelland, J.-E. Iversen, K. Moenig, and K. Lekvam. "Feasibility Study for the Use of Kinetic Hydrate Inhibitors in Deep-Water Drilling Fluids,." *Energy Fuels* **2008**, 22: 2405.
(36) L. D. Talley, G. F. Mitchell, and R. H. Oelfke. *Ann. N. Y. Acad. Sci.* **2000**, 912: 314.
(37) D. L. Crosby, G. T. Rivers, and L. M. Frostman. International Patent Application WO/2005/116399.

Chapter 2. THF-hydrate Crystal Growth Test

This thesis aimed to synthesize and test new chemicals to see their inhibition of THF hydrate on a THF rig. THF hydrates, the THF hydrate crystal growth test procedure, and the practical use of this test will all be discussed in this chapter.

2.1 THF Hydrates

Tetrahydrofuran (THF) is a polar organic liquid soluble in polar and non-polar chemicals. The THF molecule has a five-sided cyclic ether structure with the formula $(CH_2)_4O$ (Figure 2.1). It has drawn much attention in the literature due to its qualities as an organic solvent and its ability to hydrate into structure II without needing high pressure when it comes in contact with water under 4.4 °C. When combined, THF and water create homogeneous liquid mixtures across the whole composition range because THF and water are entirely miscible in the liquid state under ambient circumstances.[1, 2]

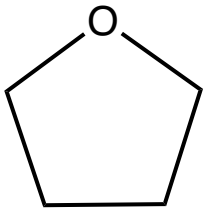

Figure 2.1 Tetrahydrofuran $(CH_2)_4O$

Structure II is the most common gas hydrate structure in the oil and gas industry.[3] Since THF creates this structure, a test method has been developed to see if a potential chemical can prevent the formation of THF hydrates without needing high pressure. THF is water-soluble, so the inhibition mechanism differs from real gas hydrate systems. However, this method can still indicate how a chemical inhibits the growth of THF hydrate crystals but not nucleation inhibition. When finding potential chemicals that can inhibit the growth of THF hydrate crystals, the chemical must be able to absorb onto the hydrate's surface to block further hydrate formation. This is one of the main mechanisms of a KHI, but if the KHI mechanism is to stop the nucleation of gas hydrates, this method is unreliable.[4] Chemicals that work well as CGIs on the THF rig can be further tested as LDHIs, either as a KHI, an AA, or a synergist with other commercially used polymers (KHIs) to inhibit nucleation of gas hydrates.

2.2 THF Hydrate Crystal Growth Experimental Procedure

In this thesis, various organic compounds, including tertiary amine oxides and amine oxides with ring structures, with either cycloalkyl or heterocyclic groups, were tested. The objective was to see how well these compounds would inhibit THF hydrate crystal growth. The tests were conducted in the laboratory with a THF rig, as seen in Figure 2.2. The THF rig consists of a cooling bath, where a cooling system controls the temperature. The mixture contains water and a small amount of glycol, which prevents the water from freezing. This cooling bath is topped with a metal apparatus with holes in the bottom for the chemical-filled THF solution's beakers. As a result, when the tests are running, the beakers can reach the same temperature as the cooling bath. During the test, a metal plate secures the glass tubes filled with ice crystals at the top of the sets. More details are provided below.

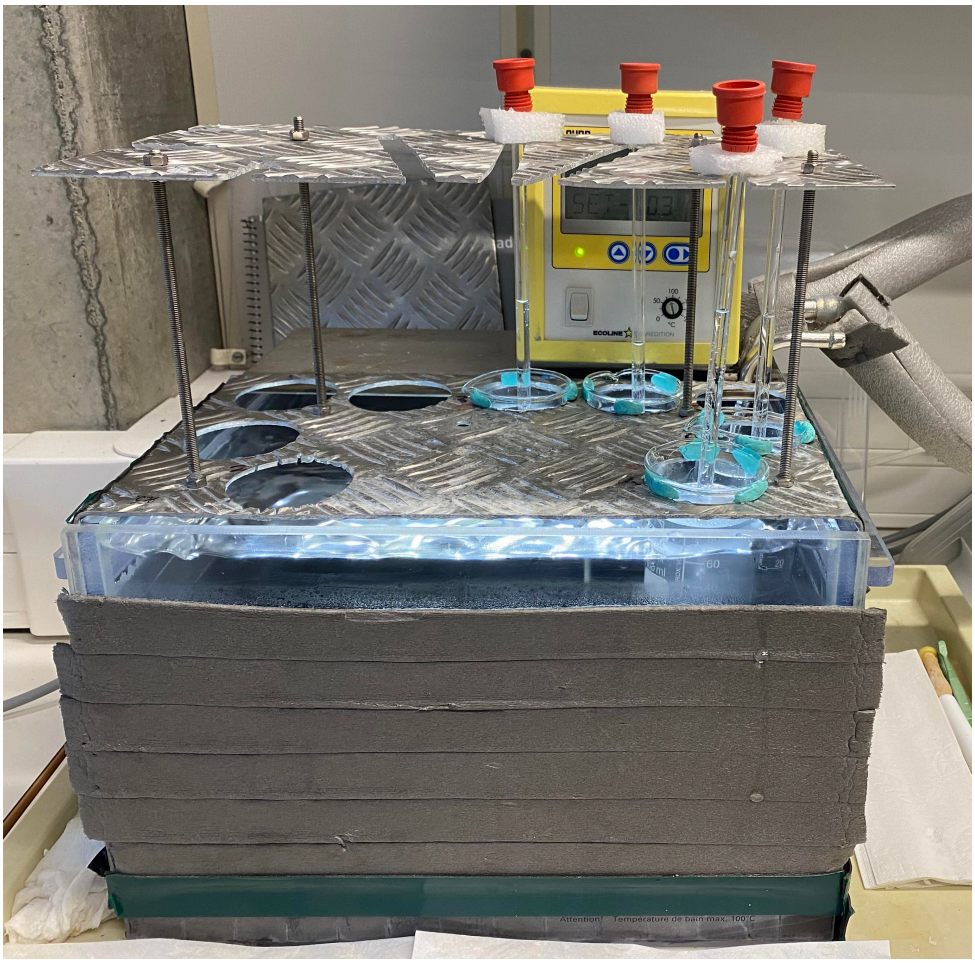

Figure 2.2 THF rig with four ongoing tests.

2.2.1 Test Procedure for THF Hydrate Crystal Growth

A mixture of sodium chloride (26.28 g) and THF (99.9%, 170 g) were added to a 1.0 L glass beaker. Deionized water was then added to create a final volume of 900 mL. The stoichiometrically correct molar composition for the formation of structure II THF hydrate, $THF \cdot 17H_2O$, was provided by this mixture. The equilibrium temperature for structure II THF hydrate formation is 4.4 °C. However, the added salt reduces the temperature to roughly 3.3 °C. The following test procedure was used to determine the crystal growth inhibition of THF hydrate with an additive: [5–7]

1. The test chemical was placed in a 100 mL glass beaker and dissolved in 80 mL THF/NaCl aqueous solution. The following amount of chemicals was used; 0.32 g, 0.16g, and 0.08 g, which gave the following concentrations: 4000 ppm, 2000 ppm, and 1000 ppm.
2. The glass beaker was then placed in a preset cooling bath at -0.3 °C (± 0.05°C), corresponding to a subcooling of 3.6 °C. Temperatures below zero are needed to prevent the ice in the glass tubes from melting. And without the salt, the subcooling would be so great that the crystal formation would develop too quickly. It would have been difficult to see the difference in performance between the chemicals.
3. The solution in the beakers was stirred every 5 minutes for 20 minutes. That is when the temperature of the solution reached -0.3 °C.
4. The end of a glass tube was then filled with ice crystals kept at -10 °C.
5. The glass tube containing ice crystals was placed in the THF/NaCl/chemical solution. They were used to initiate the THF hydrate formation.
6. The THF hydrate crystals were allowed to form at the end of the tube in the solution for 60 minutes.
7. The glass tube was then removed, and the THF hydrate crystals formed at the end of the tube were cut off with a knife and weighed. The THF hydrate crystal growth inhibition rate was measured in grams per hour.

2.2.1.1 Reference Results

A few tests were conducted and served as reference results for comparison with those of the chemical compounds created in the following chapter. Tests were run with well-known crystal growth inhibitors such as TBAB and TPAB, as well as without additives. Table 2.1 displays the findings. The THF rig's test conditions were the same for each experiment.

Table 2.1 THF Hydrate Crystal Growth Rate (g/h) at -0.3 °C for no additives, TBAB, and TPAB, measured for 1 hour with the following concentrations (ppm): 4000 and 2000.

Chemical tested/ test date	Concentration (ppm)	Growth (gram/ hour)	Average growth (gram/ hour)	Comments
No additive/ 17.01.23, 15.04.23	------	1.9, 1.3, 2.2, 1.9, 1.738, 1.749, 2.385, 1.153	1.70	Pyramid formed crystals
TBAB/ 19.01.23, 14.03.23	4000	0.48, 0.47, 0.44, 0.32, 0.273, 0.358	0.39	Pyramid formed crystals
23.01.23, 14.03.23	2000	0.897, 0.766, 0.583, 1.141, 0.593, 0.630	0.76	Pyramid formed crystals
TPAB/ 19.01.23, 14.03.23	4000	0.03, 0.023, 0.018, 0.0, 0.008, 0.017	0.01	Almost no crystal growth
23.01.23, 14.03.23	2000	0.286, 0.016, 0.044, 0.029, 0.313, 0.162	0.14	

2.2.2 Test Procedure for Branched vs. Linear Polymers

The limiting concentration for zero growth (LCZG) was determined when comparing the effectiveness of branched polymers versus linear polymers in inhibiting the growth of THF hydrate crystals. The procedure for determining the LCZG for the various polymers was almost identical to the one used in 2.2.1. Instead of measuring the weight of the crystals after 1 hour, the concentration that totally prevented all growth in 1 hour (LCZG) was measured.[8] If crystals did form, the crystals usually could not be weighed as they were in the form of thin plates that reached the beaker walls. In such cases, the polymer concentration was increased until the nearest 100 ppm of LCZG was determined. If there was no THF hydrate in the first test, the concentration of the additive was decreased until crystals did form. Thus, the LCZG can be approached from concentrations both above and below this value.

2.3 References

(1) Herslund, P. J.; Thomsen, K.; Abildskov, J.; von Solms, N.; Galfré, A.; Brântuas, P.; Kwaterski, M.; Herri, J.-M. Thermodynamic Promotion of Carbon Dioxide–Clathrate Hydrate Formation by Tetrahydrofuran, Cyclopentane and Their Mixtures. *Int. J. Greenh. Gas Control* **2013**, *17*, 397–410. https://doi.org/10.1016/j.ijggc.2013.05.022.

(2) Kelland, M. A.; Kvæstad, A. H.; Astad, E. L. Tetrahydrofuran Hydrate Crystal Growth Inhibition by Trialkylamine Oxides and Synergism with the Gas Kinetic Hydrate Inhibitor Poly(N-Vinyl Caprolactam). *Energy Fuels* **2012**, *26* (7), 4454–4464. https://doi.org/10.1021/ef300624s.

(3) Kelland, M. A. *Production Chemicals for the Oil and Gas Industry*, 2nd ed.; CRC Press, 2014.

(4) L. D. Talley, G. F. Mitchell, and R. H. Oelfke. *Ann. N. Y. Acad. Sci.* **2000**, 912: 314.

(5) U. C. Klomp, V. C. Kruka, and R. Reijnhart. WO Patent Application 95/17579. **1995**.

(6) Kelland, M. A.; Mady, M. F. Acylamide and Amine Oxide Derivatives of Linear and Hyperbranched Polyethylenimines. Part 1: Comparison of Tetrahydrofuran Hydrate Crystal Growth Inhibition Performance. *Energy Fuels* **2016**, *30* (5), 3934–3940. https://doi.org/10.1021/acs.energyfuels.6b00386.

(7) Norland, A. K.; Kelland, M. A. Crystal Growth Inhibition of Tetrahydrofuran Hydrate with Bis- and Polyquaternary Ammonium Salts. *Chem. Eng. Sci.* **2012**, *69* (1), 483–491. https://doi.org/10.1016/j.ces.2011.11.003.

(8) O'Reilly, R.; Ieong, N. S.; Chua, P. C.; Kelland, M. A. Crystal Growth Inhibition of Tetrahydrofuran Hydrate with Poly(N-Vinyl Piperidone) and Other Poly(N-Vinyl Lactam) Homopolymers. *Chem. Eng. Sci.* **2011**, *66* (24), 6555–6560. https://doi.org/10.1016/j.ces.2011.09.010.

Chapter 3. Amine Oxides with Ring Structures – Cycloalkyl or Heterocyclic Groups

The synthesis of various organic compounds, including trialkylamine oxides and alkylated amine oxides with ring structures, either with cycloalkyl or heterocyclic groups, will be covered in this chapter. These organic compounds are used in further experimental procedures to study if these chemicals can inhibit THF crystal growth.

3.1 Background

It is previously known that some alkylated amine oxides effectively inhibit THF crystal growth. The best alkylated amine oxides that inhibit THF crystal growth, as mentioned before, were found to be tri-n-butylamine oxide (TBAO), tri-n-pentylamine oxide (TPAO), and tri-iso-pentylamine oxide (TiPAO). They have a structural resemblance with the well-known quaternary ammonium salts tetrabutylammonium bromide (TBAB) and tetrapentylammonium bromide (TPAB), though instead of having a bromide ion and four alkyl groups attached to the nitrogen, they have three alkyl groups and a nitrogen-oxygen bond. Amine oxides may be less toxic than quaternary ammonium salts due to their nonionic character.[1] In previous studies, larger ring amine oxides like polyether cycloimine oxide with 5-7 membered rings as side chains have exhibited good KHI performance of synthetic natural gas mixture.[2] Still, smaller ring structures of amine oxides have not been investigated before now.

In this project, 5-7 membered ring structures are used. The ring structure attached to the amine oxides may act as the small gas molecules that fit inside the cages of the gas hydrates by van der Waals interactions. Then the polar amine oxide group can form a hydrogen bond with water located on the hydrates surface. Another theory is that the alkylated group synthesized to the amine act as the small gas molecule, and the non-polar part of the ring structure forms a hydrophobic barrier repelling water molecules.

3.2 Synthesis of Trialkylamine Oxides and an Alkylamine Oxide

A trialkylamine is an amine where the nitrogen atom is directly bonded to three alkyl groups. In this project, the nitrogen atom is directly bonded to either butyl, pentyl, or iso-pentyl, previously found to inhibit THF crystal growth best. These trialkyl amines were synthesized with 30 wt.% hydrogen peroxide (H_2O_2) and isopropanol to create trialkyl amine oxides. [3] They were used as reference results alongside the quaternary ammonium salts TBAB and TPAB. The general synthesis of amine oxides is shown in Figure 3.1. An alkylamine oxide was also synthesized to see if the ring structure actually possessed an optimized structure for inhibiting the THF hydrate crystal growth.

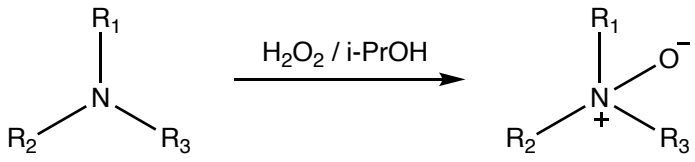

Figure 3.1 General synthesis of amine oxides. R = alkyl groups

3.2.1 Synthesis of Tri-n-butylamine oxide (TBAO)

5.008 g (27.07 mmol) of tri-n-butylamine was added to a plastic bottle. Then, 3.259 g (28.69 mmol, 1.06 mol equiv.) of 30 wt.% hydrogen peroxide was added. Next, Isopropanol (5.0 g) was added as a solvent. The reaction mixture was stirred for two days at room temperature to give a solution of tri-n-butylamine oxide with 41.39 wt.%.

3.2.2 Synthesis of Tri-n-pentylamine oxide (TPAO)

3.035 g (13.37 mmol) of tri-n-pentylamine was added to a plastic bottle with 1.681 g (14.83 mmol, 1.1 mol equiv.) of 30 wt.% hydrogen peroxide. Then, 3.0 g of isopropanol was added as a solvent. The reaction mixture was stirred at room temperature for four days to give a solution of tri-n-pentylamine oxide with 42.28 wt.%.

3.2.3 Synthesis of Tri-iso-pentylamine oxide (TiPAO)

3.024 g (13.32 mmol) of tri-iso-pentylamine was added to a plastic bottle with 1.661 g (14.65 mmol, 1.1 mol equiv.) of 30 wt.% hydrogen peroxide. Then, 3.0 gr of isopropanol was added as a solvent. The reaction mixture was stirred overnight at room temperature to give a solution of tri-iso-pentylamine oxide with 42.49 wt.%.

3.2.4 Synthesis of Di-n-butyl-4-heptylamine oxide

Step 1:
4.036 g (35.09 mmol) of 4-heptylamine, 10.188 g (74.36 mmol, 2.1 mol equiv.) of 1-bromobutane, and 10.428 g (75.57 mmol, 2.1 mol equiv.) of potassium carbonate was added to a round bottom flask with 30 ml isobutyronitrile as the solvent. The reaction mixture was refluxed at 120 °C with a stirrer for two days. The solids were dissolved using deionized water before the mixture was transferred to a separating funnel. The oil phase was washed with deionized water and isobutyronitrile three times before it was dried with anhydrous sodium sulfate and decanted into a florentine. The solvent was then evaporated on a rotovap set at 70-75 °C and 150 mbar. The yield of di-n-butyl-4-heptylamine was 4.797 g, and the solution was 96% pure, confirmed by ^{1}H-NMR. The ^{1}H-NMR spectra can be seen under the appendices.

Step 2:
A mixture of 4.797 g (21.13 mmol) di-n-butyl-4-heptylamine, 2.634 g (23.24 mmol, 1.1 mol equiv.) 30% hydrogen peroxide, and 4.7 g isopropanol used as the solvent, was stirred at room temperature overnight to get a solution of di-n-butyl-4-heptylamine oxide with 41.65 wt.%. The two-step synthesis is shown in Figure 3.2.

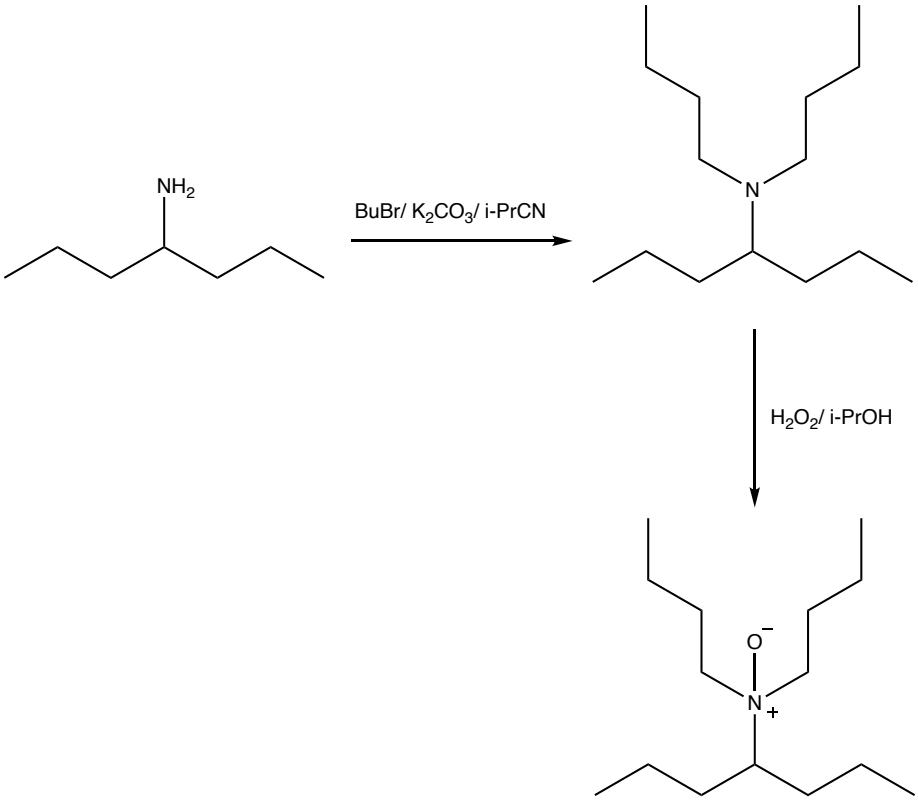

Figure 3.2 Two-step synthesis of di-n-butyl-4-heptylamine oxide.

3.3 Synthesis of Amine Oxides with cycloalkyl groups

A cycloalkyl group is a compound derived from a cycloalkane. The different ring structures used in this project were the 5-7 membered rings cyclopentyl, cyclohexyl, cycloheptyl, and cyclohexanemethylamine. The nitrogen atom was alkylated with either 1-bromobutane, 1-bromopentane, or 1-bromo-3-methylpentane. Then the compound was oxidized with 30 wt.% hydrogen peroxide (H_2O_2) and isopropanol to create the resulting cycloalkyl amine oxide used for further testing.

3.3.1 Synthesis of Di-n-butylcyclopentylamine oxide

Step 1:

2.0 g (23.53 mmol) of cyclopentylamine, 6.824 g (49.81 mmol, 2.1 mol equiv.) of 1-bromobutane, and 6.930 g (50.22 mmol, 2.1 mol equiv.) of potassium carbonate were added to a round bottom flask. Next, 30 ml of isobutyronitrile was added as the solvent. The reaction mixture was refluxed at 120 °C with a stirrer overnight. The solids were dissolved using deionized water before the mixture was transferred to a separating funnel. The oil phase was washed with deionized water and isobutyronitrile three times before it was dried with anhydrous sodium sulfate and decanted into a florentine. The solvent was then evaporated under pressure on a rotary evaporator (rotovap) set at 70 °C and 225 mbar, resulting in a 46% pure product of di-n-butylcyclopentylamine yielding 4.641 g.

Step 2:

A mixture of 4.641 g (23.55 mmol) di-n-butylcyclopentylamine, 2.935 g (25.90 mmol, 1.1 mol equiv.) of 30 wt.% hydrogen peroxide was added to the florentine, and 5.0 g of isopropanol was added as the solvent. The reaction mixture was stirred at room temperature for four days to give a solution of di-n-butylcyclopentylamine oxide with 40.4 wt.%. The two-step synthesis is shown in Figure 3.3.

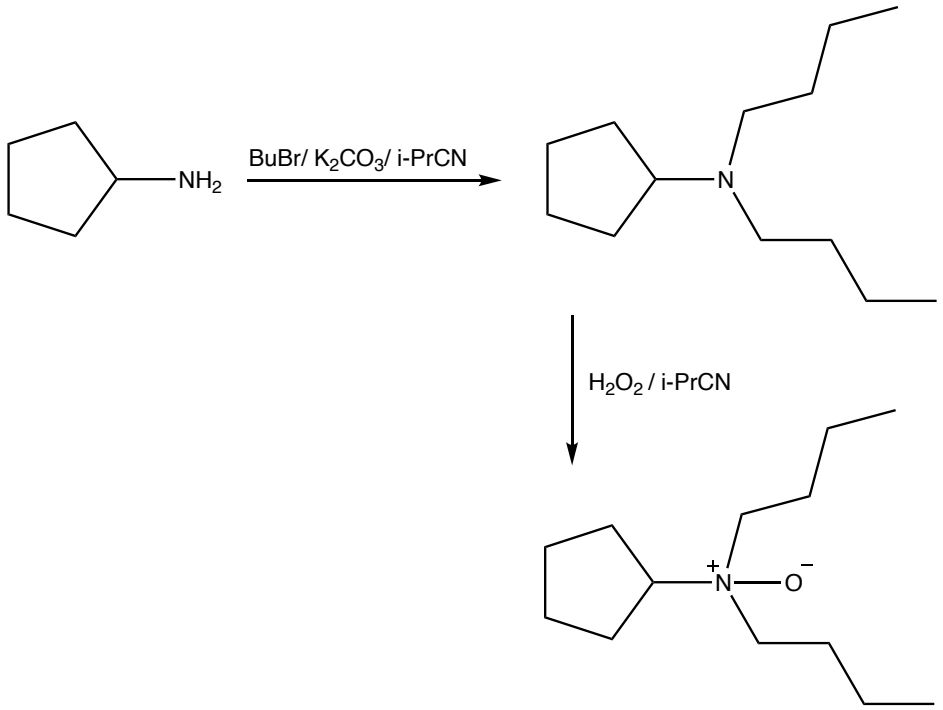

Figure 3.3 Two-step synthesis of Di-n-butylcyclopentylamine oxide.

A larger batch of di-n-butylcyclopentylamine was also made and was as follows:

Step 1:
4.045 g (47.59 mmol) of cyclopentylamine, 13.691 g (99.93 mmol, 2.1 mol equiv.) of 1-bromobutane, and 13.791 g (99.93 mmol, 2.1 mol equiv.) of potassium carbonate with 30 ml isobutyronitrile as the solvent was used to make the larger batch. The same workup was executed, but the pressure on the rotovap was changed to 150 mbar to evaporate more of the isobutyronitrile. This yielded 5.808 g of 89 % pure di-n-butylcyclopentylamine, confirmed by ^{1}H-NMR. The ^{1}H-NMR spectra can be seen under the appendices. There was still 11% isobutyronitrile in the product.

Step 2:
A mixture of 5.808 g (29.48 mmol) of di-n-butylcyclopentylamine, 3.675 g (32.43 mmol, 1.1 mol equiv.) of 30% hydrogen peroxide, and 6.0 g isopropanol were stirred at room temperature for 11 days to give a product of Di-n-butylcyclopentylamine oxide with 41.5 wt.%.

3.3.2 Synthesis of Di-n-butylcyclohexylamine oxide

Step 1:
2.103 g (21.24 mmol) of cyclohexylamine, 6.111 g (44.61 mmol, 2.1 mol equiv.) of 1-bromobutane, and 6.156 g (44.61 mmol, 2.1 mol equiv.) of potassium carbonate was added to a round bottom flask. Then, 30 ml of isobutyronitrile was added as the solvent. The reaction mixture was refluxed at 120 °C with a stirrer overnight. The same procedure described in 3.3.1 was followed. The solvent was then evaporated on a rotovap set at 70-75 °C and 150 mbar. The yield of di-n-butylcyclohexylamine was 3.761 g, and the solution was >95% pure, confirmed by ^{1}H-NMR. The ^{1}H-NMR spectra can be seen under the appendices.

Step 2:
3.761 g (17.82 mmol) of di-n-butylcyclohexylamine, 2.222 g (19.61 mmol, 1.1 mol equiv.) of 30% hydrogen peroxide and 3.0 g isopropanol as the solvent was stirred at room temperature for four days to give a solution of di-n-butylcyclohexylamine oxide with 41.91 wt.%. The two-step synthesis is shown in Figure 3.4.

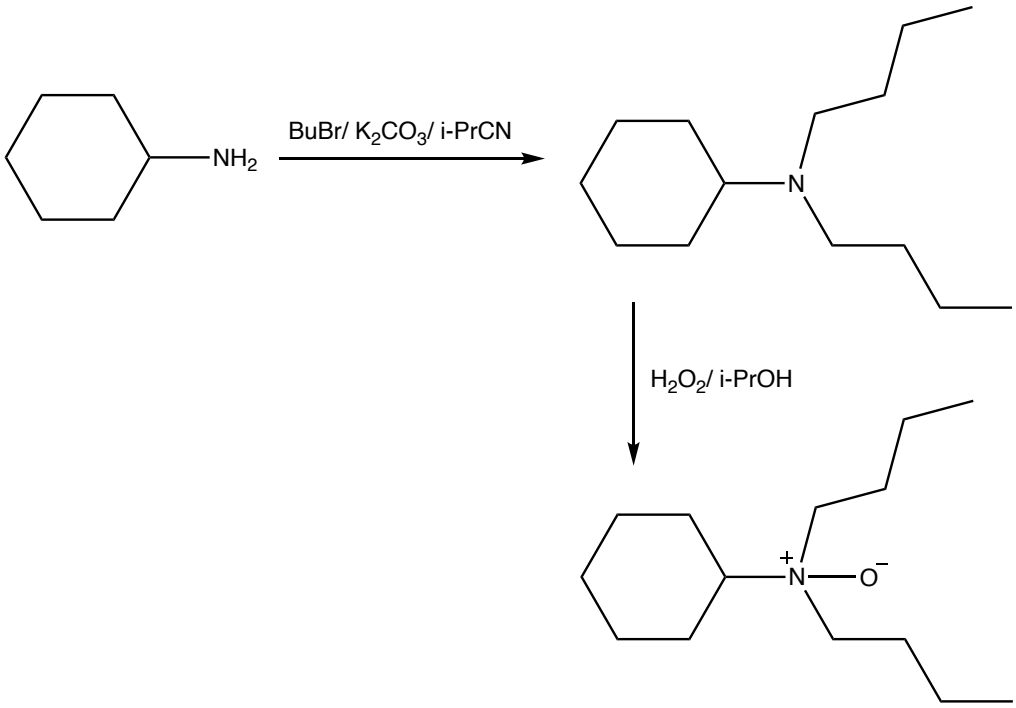

Figure 3.4 Two-step synthesis of Di-n-butylcyclohexylamine oxide.

A larger batch of di-n-butylcyclohexylamine oxide was also made and was as follows:

Step 1:

8.0 g (80.82 mmol) of cyclohexylamine, 23.63 g (172.5 mmol, 2.1 mol equiv.) of 1-bromobutane, 23.71 g (171.8 mmol, 2.1 mol equiv.) of potassium carbonate was added to a round bottom flask with 50 ml isobutyronitrile as the solvent. The reaction mixture was refluxed at 120 °C with a stirrer overnight. The same procedure described in 3.3.1 was followed. The solvent was then evaporated on a rotovap set at 70-75 °C and 150 mbar. This gave a 95% pure di-n-butylcyclohexylamine solution, confirmed by ^{1}H-NMR, with a 10.211 g yield. The ^{1}H-NMR spectra can be seen under the appendices.

Step 2:

10.211 g (48.39 mmol) of di-n-butylcyclohexylamine, 6.033 g (53.23 mmol, 1.1 mol equiv.) of 30% hydrogen peroxide, and 10.0 g of isopropanol as the solvent was stirred at room temperature for two days. This gave a solution of di-n-butylcyclohexylamine oxide with 44.02 wt.%.

3.3.3 Synthesis of Di-n-butylcycloheptylamine oxide

Step 1:

3.088 g (27.33 mmol) of cycloheptylamine, 7.882 g (57.53 mmol, 2.1 mol equiv.) of 1-bromobutane, and 7.934 g (57.49 mmol, 2.1 mol equiv.) of potassium carbonate was added to a round bottom flask. 30 ml isobutyronitrile was added as the solvent. The reaction mixture was refluxed at 120 °C with a stirrer overnight. The same procedure described in 3.3.1 was followed. The solvent was then evaporated on a rotovap set at 70-75 °C and 150 mbar. This yielded 5.247 g of 73 % pure di-n-butylcycloheptylamine, confirmed by ^{1}H-NMR. The ^{1}H-NMR spectra can be seen under the appendices.

Step 2:

A mixture of 5.247g (23.32 mmol) di-n-butylcycloheptylamine, 6.033 g (53.23 mmol, 1.1 mol equiv.) 30% hydrogen peroxide, and 10.0 g isopropanol as the solvent was stirred for two days in room temperature to give a 44.02 wt.% solution of di-n-butylcycloheptylamine oxide. The two-step synthesis is shown in Figure 3.5.

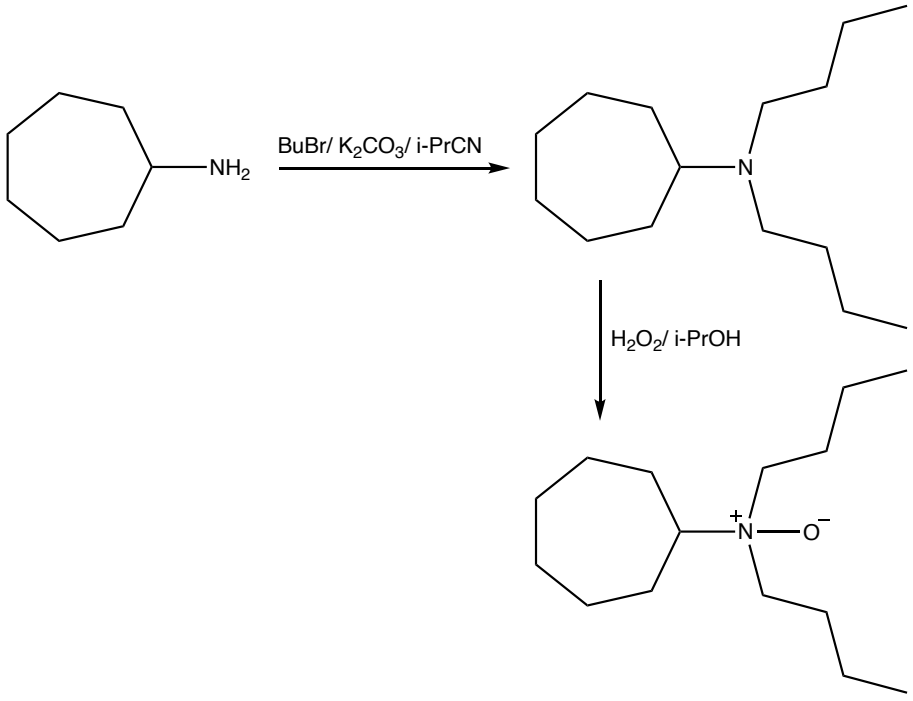

Figure 3.5 Two-step synthesis of Di-n-butylcycloheptylamine oxide.

A larger batch of di-n-butylcycloheptylamine oxide was also made and was as follows:

Step 1:
8.023 g (71.0 mmol) of cycloheptylamine, 20.464 g (149.4 mmol, 2.1 mol equiv.) of 1-bromobutane, and 20.582 g (149.1 mmol, 2.1 mol equiv.) of potassium carbonate was added to a round bottom flask. 50 ml of isobutyronitrile was added as the solvent, and the reaction mixture was refluxed at 120 °C with a stirrer overnight. The same procedure described in 3.3.1 was followed. The solvent was then evaporated on a rotovap set at 70-75 °C and 150 mbar. This gave a 95% pure di-n-butylcycloheptylamine, confirmed by ^{1}H-NMR, with a 13.747 g yield. The ^{1}H-NMR spectra can be seen under the appendices.

Step 2:
13.747 g (61.10 mmol) of di-n-butylcycloheptylamine, 7.687 g (67.83 mmol, 1.1 mol equiv.) of 30% hydrogen peroxide, and 13.0 g isopropanol was stirred at room temperature overnight to give a solution of di-n-butylcycloheptylamine oxide with 42.01 wt.%

3.3.4 Synthesis of Di-n-pentylcyclohexylamine oxide

Step 1:
1.81 g (18.28 mmol) of cyclohexylamine, 5.80 g (38.41 mmol, 2.1 mol equiv.) of 1-bromopentane, and 5.30 g (38.41 mmol, 2.1 mol equiv.) of potassium carbonate was added to a round bottom flask with 30 ml isobutyronitrile as the solvent. The reaction mixture was refluxed at 120 °C with a stirrer overnight. The same procedure described in 3.3.1 was followed. The solvent was then evaporated on a rotovap set at 70-75 °C and 150 mbar. This gave a 95% pure solution of di-n-pentylcyclohexylamine, confirmed by ^{1}H-NMR, with a 2.261 g yield. The ^{1}H-NMR spectra can be seen under the appendices.

Step 2:
2.261g (9.46 mmol) of di-n-pentylcyclohexylamine, 1.218 g (10.75 mmol, 1.1 mol equiv.) of 30% hydrogen peroxide, and 2.2 g isopropanol as the solvent was stirred for five days in room temperature to give a 42.64 wt.% solution of di-n-pentylcyclohexylamine oxide. The two-step synthesis is shown in Figure 3.6.

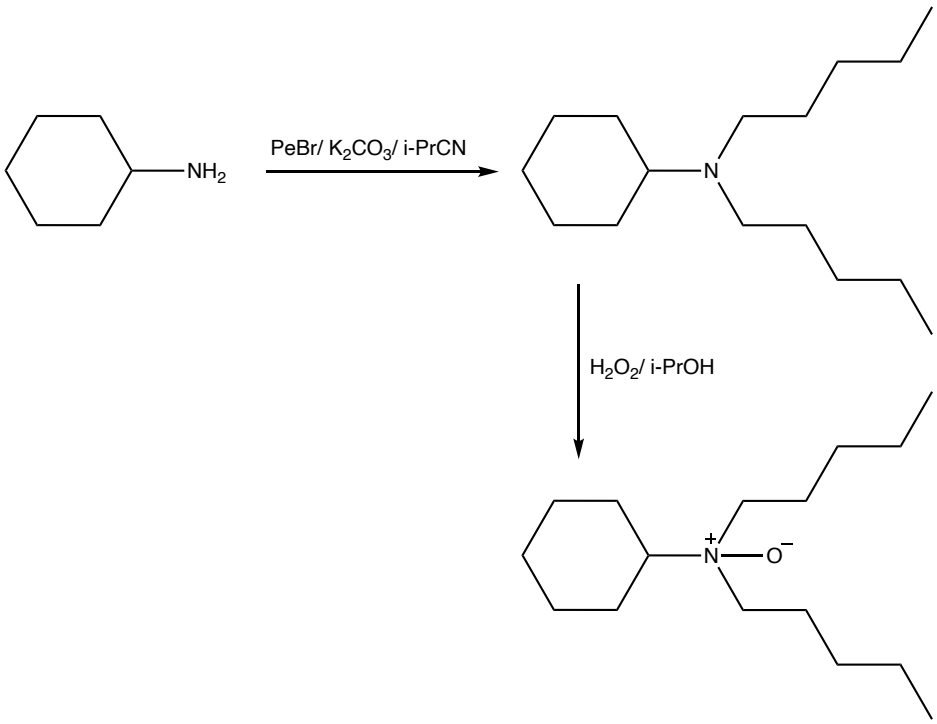

Figure 3.6 Two-step synthesis of Di-n-pentylcyclohexylamine oxide.

3.3.5 Synthesis of Di-n-pentylcycloheptylamine oxide

Step 1:

3.028 g (26.79 mmol) of cycloheptylamine, 8.561g (56.69 mmol, 2.1 mol equiv.) of 1-bromopentane, and 7.876 g (57.07 mmol, 2.1 mol equiv.) of potassium carbonate was added to a round bottom flask. 30 ml isobutyronitrile was added as the solvent. The reaction mixture was refluxed at 120 °C with a stirrer overnight. The same procedure described in 3.3.1 was followed. The solvent was then evaporated on a rotovap set at 70-75 °C and 150 mbar. This gave a 90% pure di-n-pentylcycloheptylamine, confirmed by ^{1}H-NMR, with a 4.353 g yield. The ^{1}H-NMR spectra can be seen under the appendices.

Step 2:

A mixture of 4.353 g (17.21 mmol) di-n-pentylcycloheptylamine, 2.198 g (19.39 mmol, 1.1 mol equiv.) 30 % hydrogen peroxide, and 4.3 g isopropanol used as the solvent, was stirred in room temperature for two days to get a solution of di-n-pentylcycloheptylamine oxide with 42.45 wt.%. The two-step synthesis is shown in Figure 3.7.

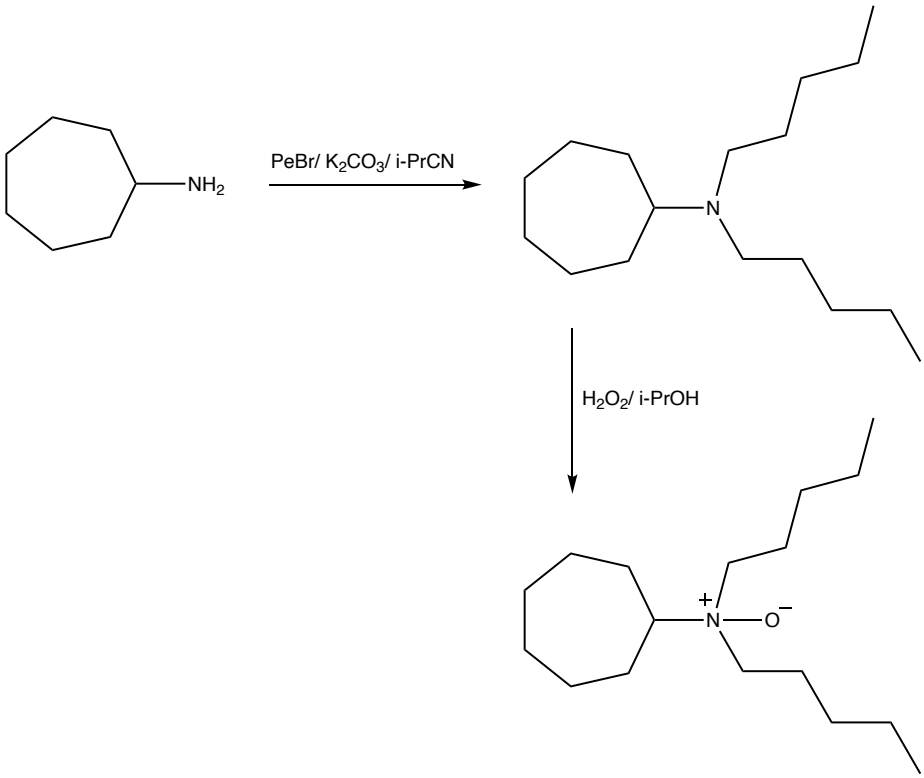

Figure 3.7 Two-step synthesis of Di-n-pentylcycloheptylamine oxide

3.3.6 Synthesis of Di-iso-pentylcycloheptylamine oxide

Step 1:

3.021 g (26.73 mmol) of cycloheptylamine, 8.479g (56.15 mmol, 2.1 mol equiv.) of 1-bromo-3-methylpentane, and 7.771 g (56.31 mmol, 2.1 mol equiv.) of potassium carbonate was added to a round bottom flask with 30 ml isobutyronitrile as the solvent. The reaction mixture was refluxed at 120 °C with a stirrer for two days. The same procedure described in 3.3.1 was followed. The solvent was then evaporated on a rotovap set at 70-75 °C and 150 mbar. This gave a 92% pure solution of di-iso-pentylcycloheptylamine, confirmed by ^{1}H-NMR, with a 4.127 g yield. The ^{1}H-NMR spectra can be seen under the appendices.

Step 2:

4.127g (16.31 mmol) of di-iso-pentylcycloheptylamine, 2.046 g (18.05 mmol, 1.1 mol equiv.) of 30% hydrogen peroxide, and 4.0 g of isopropanol used as the solvent was stirred for four days in room temperature to give a 43.01 wt.% solution of di-iso-pentylcycloheptylamine oxide. The two-step synthesis is shown in Figure 3.8.

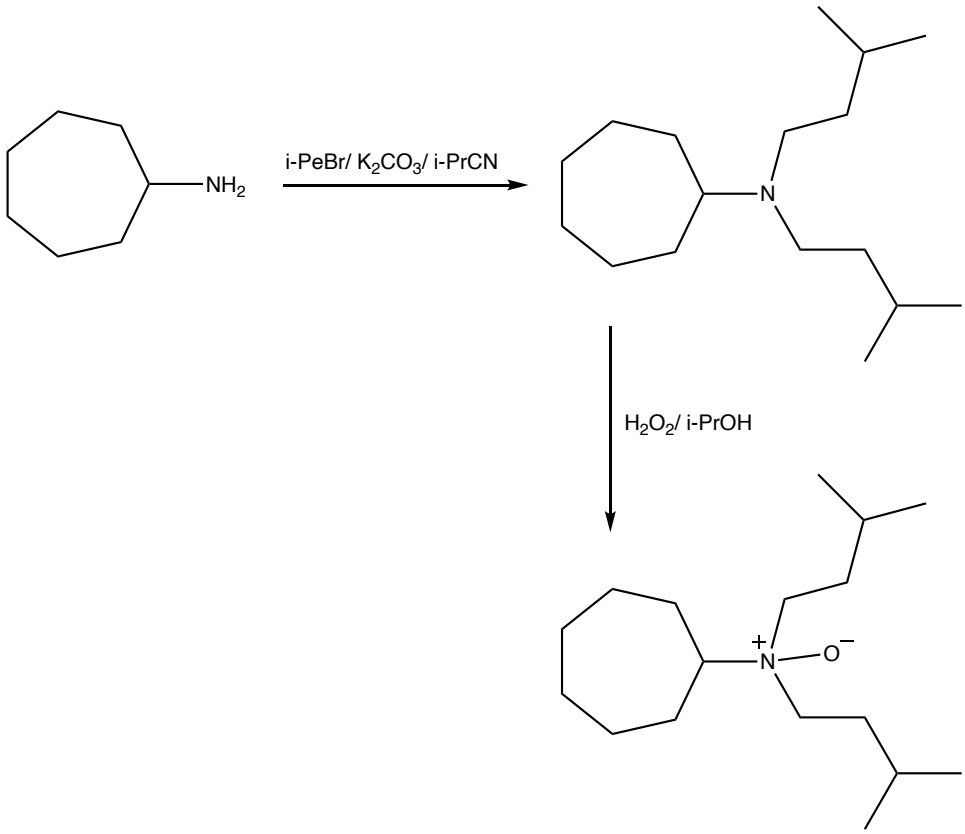

Figure 3.8 Two-step synthesis of Di-iso-pentylcycloheptylamine oxide

3.3.7 Synthesis of N-butyldicyclopentylamine oxide

Step 1:

6.002 g (40.28 mmol, 2 mol equiv.) of bromocyclopentane, 1.467 g (20.10 mmol, 1 mol equiv.) butylamine, 5.547 g (40.2 mmol, 2 mol equiv.) of potassium carbonate was added to a round bottom flask. 30 ml isobutyronitrile was added as the solvent. The reaction mixture was refluxed at 120 °C with a stirrer overnight. The same procedure described in 3.3.1 was followed. The solvent was then evaporated on a rotovap set at 70-75 °C and 150 mbar. This gave a 75% pure n-butyldicyclopentylamine, confirmed by ^{1}H-NMR, with a 1.518 g yield. The ^{1}H-NMR spectra can be seen under the appendices.

Step 2:

1.518 g (7.26 mmol) of n-butyldicyclopentylamine, 0.905 g (7.98 mmol, 1.1 mol equiv.) of 30% hydrogen peroxide, and 2.0 g isopropanol used as the solvent, was stirred at room

temperature for two days to get a solution of n-butyldicyclopentylamine oxide with 36.97 wt.%. The two-step synthesis is shown in Figure 3.9.

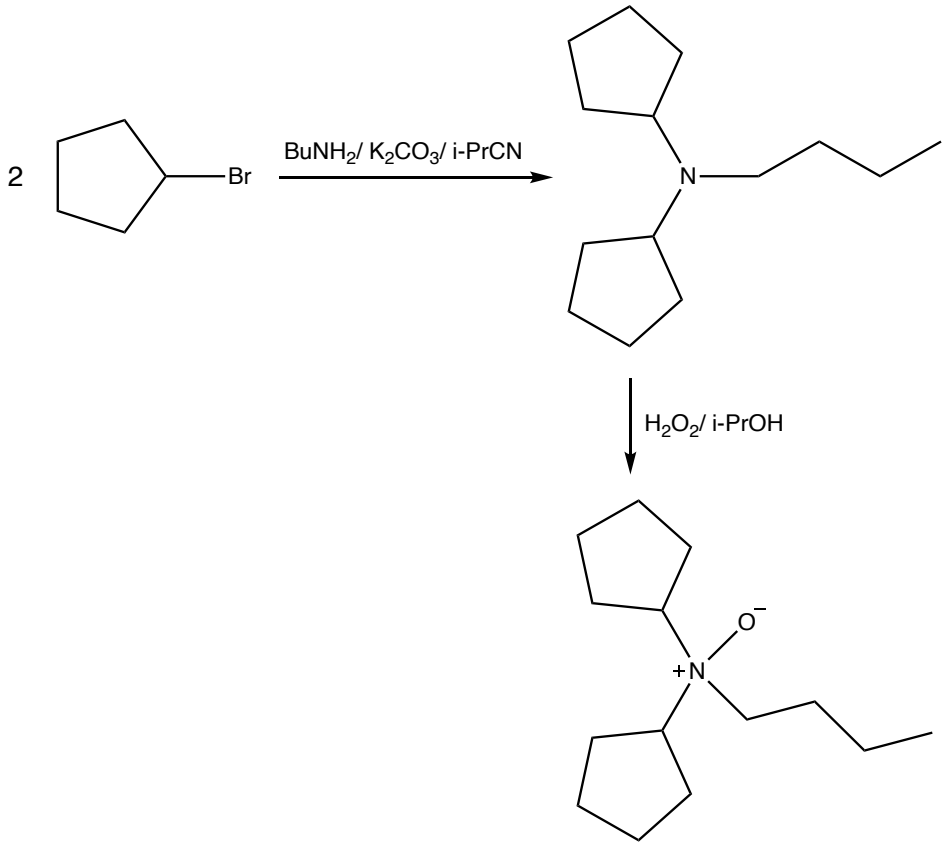

Figure 3.9 Two-step synthesis of N-butyldicyclopentylamine oxide

3.3.8 Synthesis of N-butyldicyclohexylamine oxide

Step 1:

6.031 g (33.32 mmol) of dicyclohexylamine, 4.793 g (34.99 mmol, 1.05 mol equiv.) of 1-bromobutane, and 4.828g (34.99 mmol, 1.05 mol equiv.) of potassium carbonate was added to a round bottom flask with 30 ml isobutyronitrile as the solvent. The reaction mixture was refluxed at 120 °C with a stirrer for two days. The same procedure described in 3.3.1 was followed. The solvent was then evaporated on a rotovap set at 70-75 °C and 150 mbar. The yield of n-butyldicyclohexylamine was 3.167 g, and the solution was 96% pure, confirmed by ^{1}H-NMR. The ^{1}H-NMR spectra can be seen under the appendices.

Step 2:

A mixture of 3.167 g (13.36 mmol) n-butyldicyclohexylamine, 1.666 g (14.70 mmol, 1.1 mol equiv.) 30% hydrogen peroxide, and 3.1 g of isopropanol used as the solvent, was stirred at room temperature for three days to get a solution of n-butyldicyclohexylamine oxide with 30.46 wt.%. The two-step synthesis is shown in Figure 3.10.

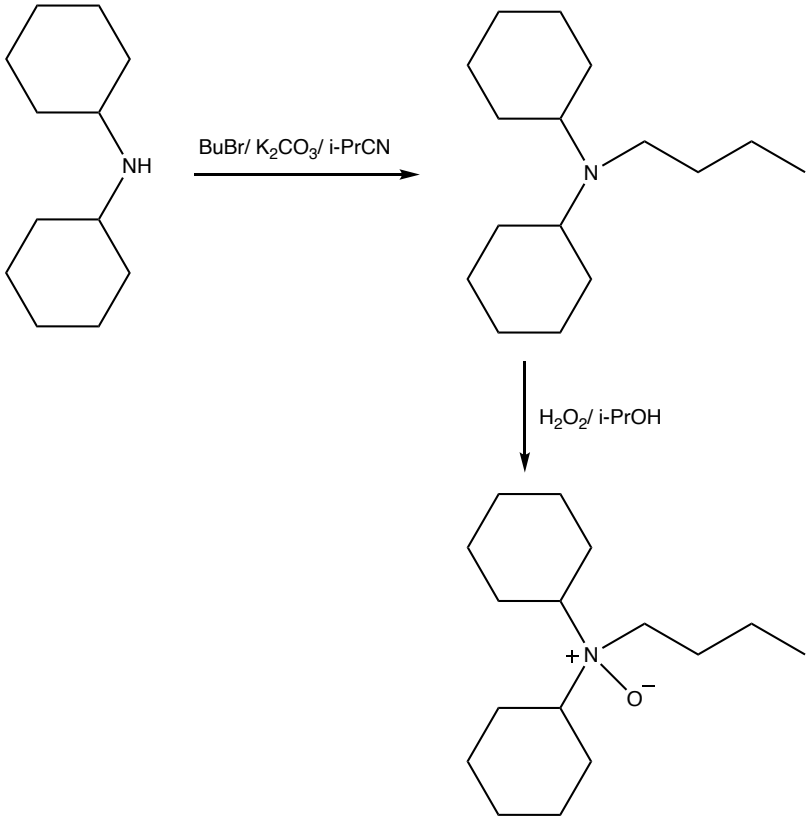

Figure 3.10 Two-step synthesis of N-butyldicyclohexylamine oxide.

3.3.9 Synthesis of Di-n-butylcyclohexanemethylamine oxide

Step 1:

3.019 g (26.72 mmol) of cyclohexanemethylamine, 7.686 g (56.10 mmol, 2.1 mol equiv.) of 1-bromobutane, and 7.743 g (56.10 mmol, 2.1 mol equiv.) of potassium carbonate was added to a round bottom flask. 30 ml isobutyronitrile was added as the solvent. The reaction mixture was refluxed at 120 °C with a stirrer overnight. The same procedure described in 3.3.1 was followed. The solvent was then evaporated on a rotovap set at 70-75 °C and 150 mbar. This gave a 96%

pure di-n-butylcyclohexanemethylamine, confirmed by ^{1}H-NMR, with a 3.885 g yield. The ^{1}H-NMR spectra can be seen under the appendices.

Step 2:
3.885 g (17.26 mmol) of di-n-butylcyclohexanemethylamine, 2.153 g (18.99 mmol, 1.1 mol equiv.) of 30% hydrogen peroxide, and 4.0 g isopropanol used as the solvent, was stirred at room temperature for two days to get a solution of di-n-butylcyclohexanemethylamine oxide with 41.56 wt.%. The two-step synthesis is shown in Figure 3.11.

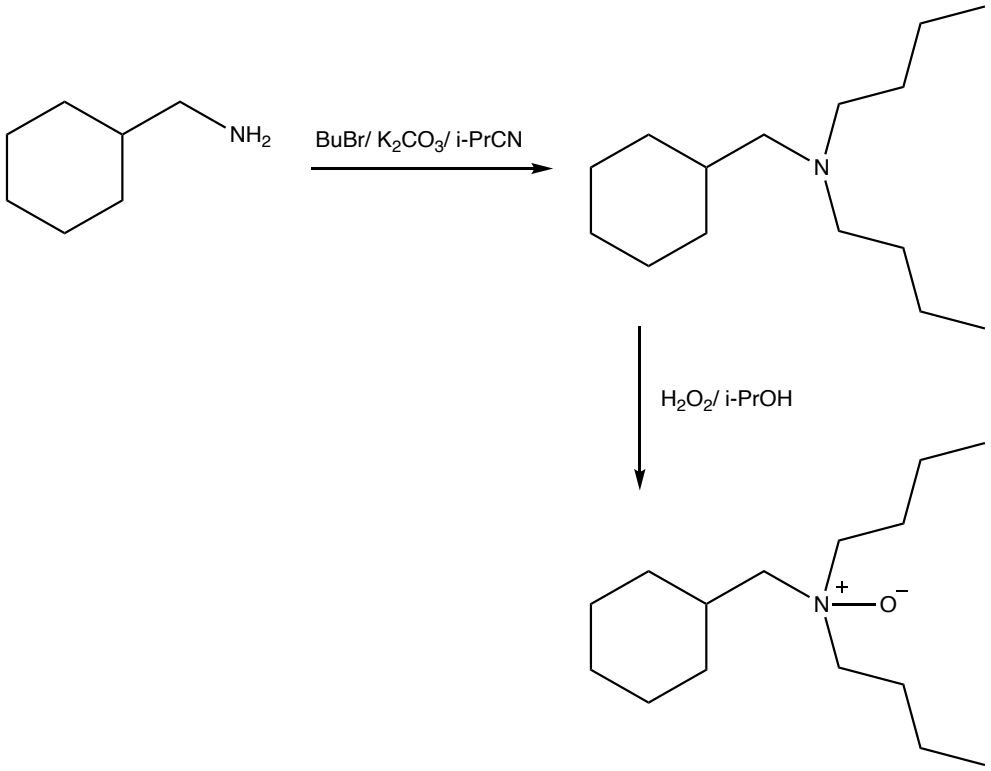

Figure 3.11 Two-step synthesis of Di-n-butylcyclohexanemethylamine oxide.

3.4 Synthesis of Amine Oxides with heterocyclic groups

A heterocyclic group consists of at least two elements with at least one amine. In this project, the 5-7 membered rings pyrrolidine, piperidine, hexamethyleneimine, methylpiperazine, and tetrahydrofurfurylamine were alkylated with 1-bromobutane. Then, the compound was oxidized with 30 wt.% hydrogen peroxide (H_2O_2) and isopropanol to create the resulting heterocyclic amine oxide used for further testing.

3.4.1 Synthesis of N-butylpyrrolidine oxide

Step 1:

4.0 grams (56.33 mmol) of pyrrolidine was placed in a round bottom flask with 8.0 grams (58.4 mmol, 1.04 equiv.) of 1-bromobutane and 8.058 grams (58.4 mmol, 1.04 equiv.) of potassium carbonate. 30 ml of isobutyronitrile was used as the solvent. The reaction mixture was refluxed at 120 °C with a stirrer overnight. The same procedure described in 3.3.1 was followed. The solvent was then evaporated on a rotovap set at 70-75 °C and 150 mbar. This gave an 80% pure solution of n-butylpyrrolidine, confirmed by ^{1}H-NMR, with a 1.695 g yield. The ^{1}H-NMR spectra can be seen under the appendices.

Step 2:

1.675 g (13.19 mmol) of n-butylpyrrolidine, 1.888 g (16.66 mmol, 1.26 mol equiv.) of 30% hydrogen peroxide, and 2.2 g of isopropanol used as the solvent was stirred overnight in room temperature to get a solution of n-butylpyrrolidine oxide with 33.27 wt.%. The two-step synthesis is shown in Figure 3.12.

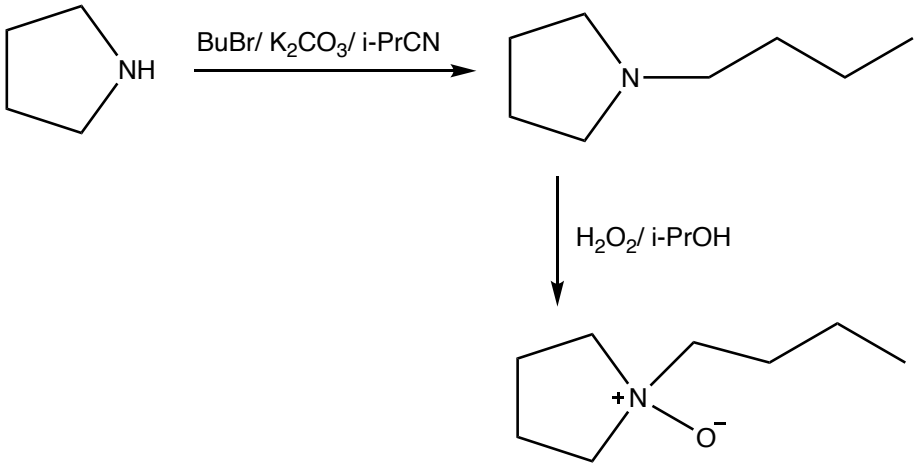

Figure 3.12 Two-step synthesis of N-butylpyrrolidine oxide.

3.4.2 Synthesis of N-butylpiperidine oxide

Step 1:

4.017 g (47.25 mmol) of piperidine, 6.798 g (49.62 mmol, 1.05 mol equiv.) of 1-bromobutane, and 6.846 g (49.61 mmol, 1.05 mol equiv.) of potassium carbonate was added to a round bottom flask with 30 ml isobutyronitrile as the solvent. The reaction mixture was refluxed at 120 °C with a stirrer overnight. The same procedure described in 3.3.1 was followed. The solvent was then evaporated on a rotovap set at 70-75 °C and 150 mbar. This gave a 2.207 g yield solution of n-piperidine. The ^{1}H-NMR spectra can be seen under the appendices.

Step 2:

A mixture of 2.177 g (15.44 mmol) n-butylpiperidine, 1.924 g (16.98 mmol, 1.1 mol equiv.) 30% hydrogen peroxide, and 2.0 g isopropanol used as the solvent, was stirred at room temperature for two days to get a solution of n-butylpiperidine oxide with 39.30 wt.%. The two-step synthesis is shown in Figure 3.13.

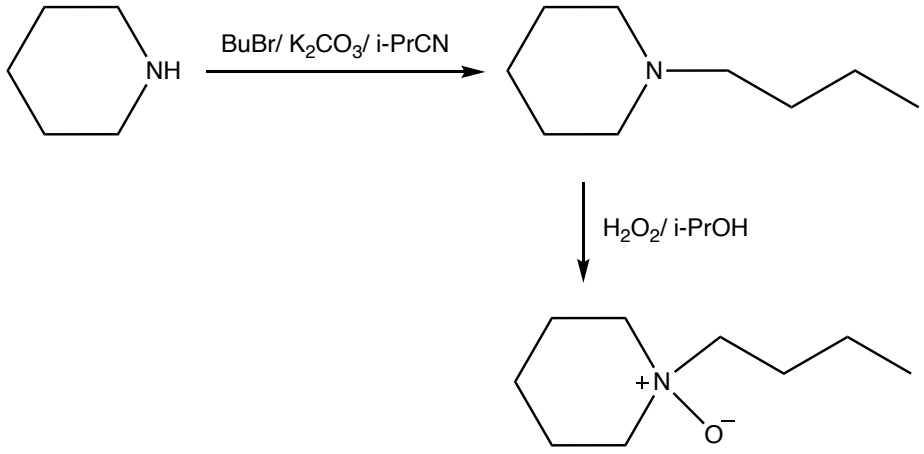

Figure 3.13 Two-step synthesis of N-butylpiperidine oxide.

3.4.3 Synthesis of N-butylhexamethyleneimine oxide

Step 1:

2.088 g (21.09 mmol) of hexamethyleneimine, 3.034 g (22.15 mmol, 1.05 mol equiv.) of 1-bromobutane, and 3.057 g (22.15 mmol, 1.05 mol equiv.) of potassium carbonate was added to a round bottom flask. 30 ml isobutyronitrile was added as the solvent. The reaction mixture was refluxed at 120 °C with a stirrer overnight. The same procedure described in 3.3.1 was followed. The solvent was then evaporated on a rotovap set at 70-75 °C and 222 mbar. The yield of n-butylhexamethyleneimine was 2.753 g, and the solution was 65% pure, confirmed by ^{1}H-NMR. The ^{1}H-NMR spectra can be seen under the appendices.

Step 2:

2.753 g (17.76 mmol) of n-butylhexamethyleneimine, 2.214 g (19.54 mmol, 1.1 mol equiv.) of 30% hydrogen peroxide, and 2.0 g of isopropanol used as the solvent was stirred overnight in room temperature to get a solution of n-butylpyrrolidine oxide with 41.30 wt.%. The two-step synthesis is shown in Figure 3.14.

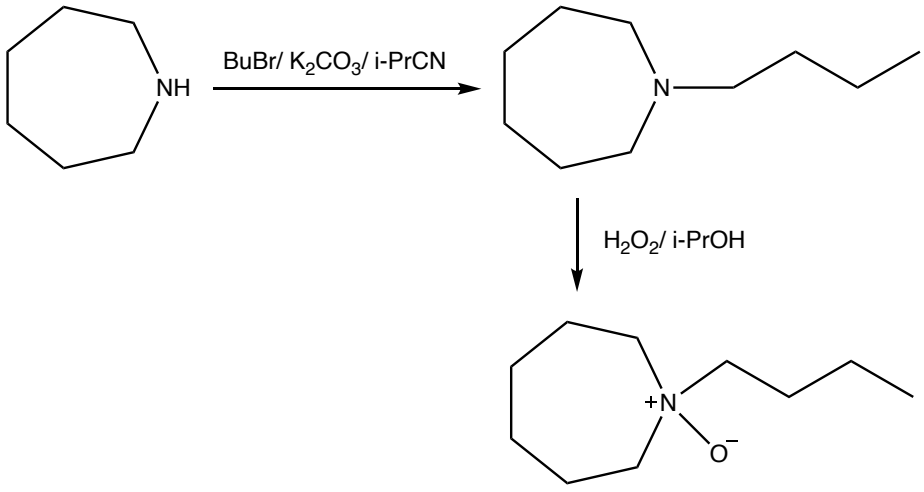

Figure 3.14 Two-step synthesis of N-butylhexamethyleneimine oxide.

3.4.4 Synthesis of Di-n-butylaminopyrrolidine oxide

3.417 g (27.89 mmol) of 1-aminopyrrolidine hydrochloride, 8.025 g (60.22 mmol, 2.1 mol equiv.) of 1-bromobutane, and 11.936 g (86.49 mmol, 3.1 mol equiv.) of potassium carbonate was added to a round bottom flask. 30 ml isobutyronitrile was added as the solvent. The reaction mixture was refluxed at 120 °C with a stirrer overnight. The same procedure described in 3.3.1 was followed. The solvent was then evaporated on a rotovap set at 70-75 °C and 150 mbar. This did not result in a pure di-n-butylaminopyrrolidine. The product had approximately 80% isobutyronitrile, so the synthesis stopped there. The ^{1}H-NMR spectra can be seen under the appendices. The synthesis is shown in Figure 3.15.

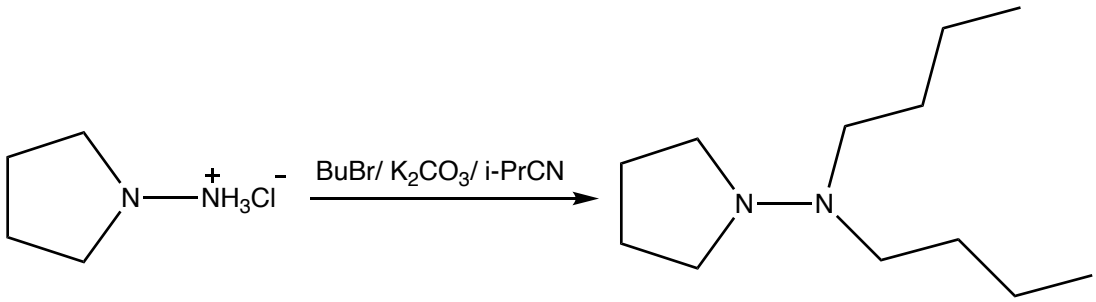

Figure 3.15 Synthesis of di-n-butylaminopyrrolidine.

3.4.5 Synthesis of 1-butyl-4-methylpiperazine oxide

Step 1:

4.018 g (40.18 mmol) of methylpiperazine, 5.780 g (42.19 mmol, 1.05 mol equiv.) of 1-bromobutane, 5.822 g (42.19 mmol, 1.05 mol equiv.) of potassium carbonate was added to a round bottom flask with 30 ml isobutyronitrile as the solvent. The reaction mixture was refluxed at 120 °C with a stirrer overnight. The same procedure described in 3.3.1 was followed. The solvent was then evaporated on a rotovap set at 70-75 °C and 150 mbar. This gave a 50% pure solution of 1-butyl-4-methylpiperazine, confirmed by ^{1}H-NMR, with a 0.969 g yield. The ^{1}H-NMR spectra can be seen under the appendices.

Step 2:

A mixture of 0.945 g (6.057 mmol) 1-butyl-4-methylpiperazine, 0.755 g (6.66 mmol, 1.1 mol equiv.) 30 % hydrogen peroxide, and 1.0 g isopropanol used as the solvent, was stirred at room temperature for two days to get a solution of 1-butyl-4-methylpiperazine oxide with 37.37 wt.%. The two-step synthesis is shown in Figure 3.16.

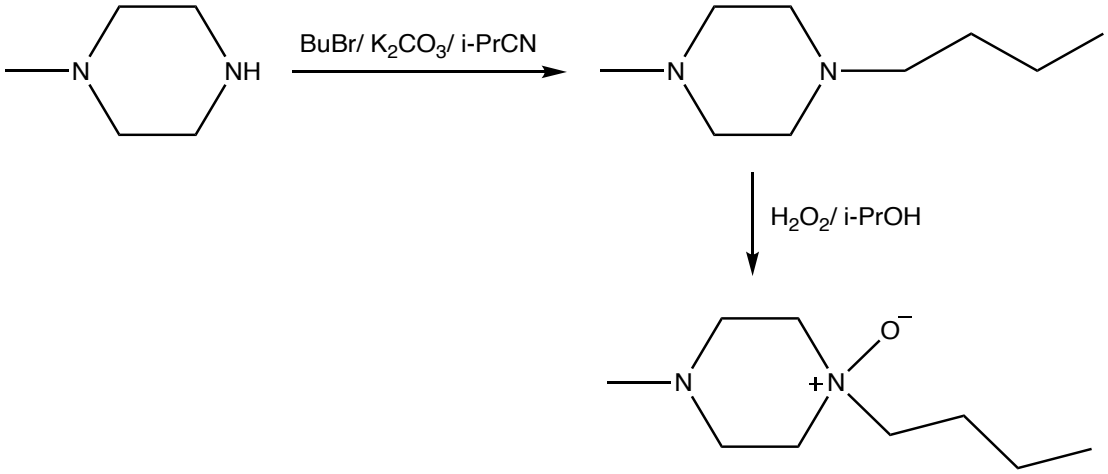

Figure 3.16. Two-step synthesis of 1-butyl-4-methylpiperazine oxide.

3.4.6 Synthesis of Di-n-butyltetrahydrofurfurylamine oxide

Step 1:

2.017 g (19.97 mmol) of tetrahydrofurfurylamine, 5.745 g (41.93 mmol, 2.1 mol equiv.) of 1-bromobutane, and 5.787 g (41.93 mmol, 2.1 mol equiv.) of potassium carbonate was added to a round bottom flask. 30 ml isobutyronitrile was added as the solvent. The reaction mixture was refluxed at 120 °C with a stirrer overnight. The same procedure described in 3.3.1 was followed. The solvent was then evaporated on a rotovap set at 70-75 °C and 222 mbar. Di-n-tetrahydrofurfurylamine yielded 3.392 g, and the solution was 85% pure, confirmed by ^{1}H-NMR. The ^{1}H-NMR spectra can be seen under the appendices.

Step 2:

3.392 g (15.92 mmol) of di-n-butyltetrahydrofurfurylamine, 1.985 g (17.51 mmol, 1.1 mol equiv.) of 30% hydrogen peroxide, and 3.5 g of isopropanol used as the solvent was stirred in

room temperature for four days to get a solution of di-n-butyltetrahydrofurfurylamine oxide with 41.62 wt.%. The two-step synthesis is shown in Figure 3.17.

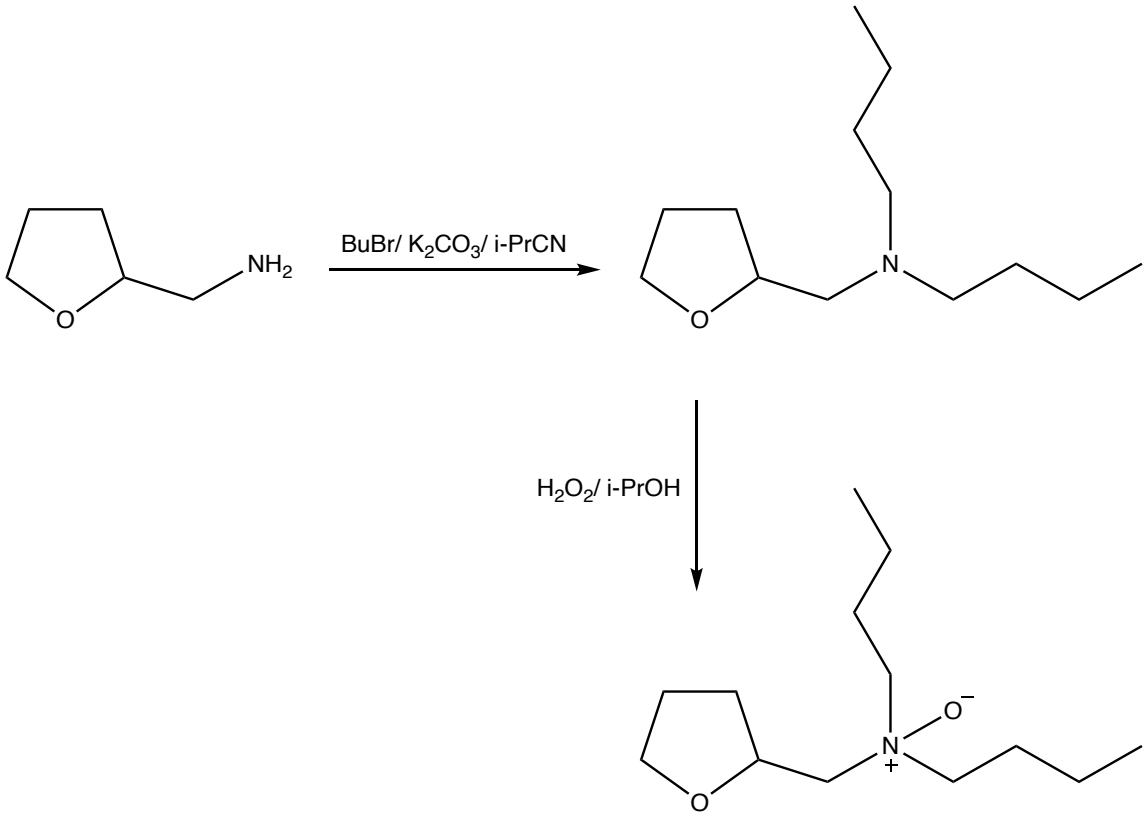

Figure 3.17. Two-step synthesis of Di-n-butyltetrahydrofurfurylamine oxide.

3.5 Results and Discussion

3.5.1 Trialkylamine Oxides and an Alkylamine Oxide

The results of the THF hydrate crystal growth rate at -0.3 °C on the THF rig with 4000, 2000, and 1000 ppm of various tertiary amine oxides are given in Table 3.1. These results, alongside the quaternary ammonium salts TBAB and TPAB, are used as reference results for the amine oxides with different ring structures.

Table 3.1. THF Hydrate Crystal Growth Rate (g/h) at -0.3 °C for Tertiary Amine Oxides measured for 1 hour with the following concentrations (ppm): 4000, 2000, 1000.

Chemical tested/ test date	Concentration (ppm)	Growth (gram/ hour)	Average growth (gram/ hour)	Comments
TBAO/ 19.01.23, 26.01.23	4000	0.011, 0.022, 0.019, 0.027, 0.020, 0.026, 0.009, 0.018	0.01	
23.01.23, 14.03.23	2000	0.138, 0.123, 0.044, 0.023, 0.013, 0.061, 0.026, 0.028	0.05	
16.02.23, 21.02.23	1000	0.486, 0.475, 0.939, 0.374, 0.538, 0.398, 0.609, 0.413	0.52	
TPAO/ 16.03.23, 21.03.23	4000	0.082, 0.033, 0.022, 0.084, 0.096, 0.060, 0.086, 0.145	0.07	
16.03.23, 28.03.23	2000	0.161, 0.309, 0.479, 0.359, 0.428, 0.144, 0.298, 0.236	0.30	
28.03.23, 30.03.23	1000	0.464, 0.531, 0.431, 0.478, 0.690, 0.498	0.51	
TiPAO/ 04.04.23, 11.04.23	4000	0.0, 0.015, 0.012, 0.004, 0.015, 0.002, 0.0, 0.004	<0.01	Almost no crystals
06.04.23, 11.04.23	2000	0.0, 0.006, 0.0, 0.008, 0.041,	0.01	Almost no crystals

		0.010, 0.018, 0.017	
11.04.23, 13.04.23	1000	0.271, 0.199, 0.192, 0.214, 0.220, 0.330, 0.371	0.25

Previous studies have determined that TBAO was the best trialkyl amine oxide THF hydrate inhibitor.[1] So, all of the synthesized ring-structured amine oxides were first alkylated with 1-bromobutane to achieve butyl groups to test the inhibition performance of the different compounds. Later in the project, TiPAO was synthesized, and the inhibiting performance appeared greater than TBAO, but the consideration of molecular weight has to be added. TiPAO has a higher molecular weight than TBAO, so if further tests had been executed with the same weight concentration, the same end result as previous studies would most likely be the case.

The results of the THF hydrate crystal growth rate at -0.3 °C on the THF rig with 4000 and 2000 ppm of Di-n-butyl-4-heptylamine oxide are shown in Table 3.2. These results are compared with Di-n-butylcycloheptylamine oxide (DBCHepAO) to see if the ring structure optimizes the inhibition.

Table 3.2 THF Hydrate Crystal Growth Rate (g/h) at -0.3 °C for Di-n-butyl-4-heptylamine oxide, measured for 1 hour with the following concentrations (ppm): 4000, 2000, 1000.

Chemical tested/ test date	Concentration (ppm)	Growth (g/h)	Average growth (g/h)	Comments
Di-n-butyl-4-heptylamine oxide/ 17.04.23, 18.04.23	4000	0.309, 0.134, 0.248, 0.221, 0.221, 0.288	0.23	Small clear oil drops.
17.04.23, 18.04.23	2000	0.989, 0.982, 1.345, 1.576, 1.198	1.20	Small clear oil drops.

3.5.2 Amine Oxides with Cycloalkyl Groups

Different amine oxides with cycloalkyl groups (e.g., cyclopentyl, cyclohexyl, and cycloheptyl) have been synthesized and tested with alkyl groups of butyl, pentyl or iso-pentyl directly bonded with the nitrogen atom of the amine. The synthesis with isobutyronitrile as the solvent had the best yield and purity of the product. We tried synthesizing the chemicals with THF as the solvent, as the vaporizing of isobutyronitrile was time-consuming, but this resulted in numerous messy products containing what seemed to be monobutylated and dibutylated compounds and unreacted 1-bromobutane mixed. This might be because of the low temperature (80 °C) under the reflux with THF that resulted in chemicals not being alkylated correctly. The THF tests were carried out on the successfully synthesized compounds to determine if the alkylated cycloalkyl amine oxides could inhibit the hydrate crystal formation of THF hydrate. If they were successful further tests would be carried out to see if they potentially could be used as both AAs and KHI synergists.

Table 3.3 shows the overview of the different cycloalkyl amine oxides tested with simplified names. These are used later on in the discussion.

Table 3.3 Overview of the various cycloalkyl amine oxides tested with simplified names.

Chemical	Simplified name
Di-n-butylcyclopentylamine oxide	DBCPAO
Di-n-butylcyclohexylamine oxide	DBCHexAO
Di-n-butylcycloheptylamine oxide	DBCHepAO
Di-n-pentylcyclohexylamine oxide	DPCHexAO
Di-n-pentylcycloheptylamine oxide	DPCHepAO
Di-iso-pentylcycloheptylamine oxide	DiPCHepAO
N-butyldicyclopentylamine oxide	BDCPAO
N-butyldicyclohexylamine oxide	BDCHAO
Di-n-butylcyclohexanemethylamine oxide	DBCHMAO

The THF hydrate crystal growth rate results at -0.3 °C on the THF rig with 4000, 2000, and 1000 ppm of the different amine oxides with cycloalkyl groups can be seen in Table 3.4. The crystal growth is measured in grams/ hour.

Table 3.4 THF Hydrate Crystal Growth Rate (g/h) at -0.3 °C for Amine Oxides with Cycloalkyl groups, measured for 1 hour with the following concentrations (ppm): 4000, 2000, 1000.

Chemical tested/ test date	Concentration (ppm)	Growth (g/h)	Average growth (g/h)	Comments
DBCPAO/ 09.03.23, 20.03.23	4000	0.117, 0.051, 0.048, 0.062, 0.076, 0.068, 0.139, 0.055	0.07	Whole crystal fell off on 0.117, 0.139
09.03.23, 20.03.23	2000	0.730, 0.295, 0.637, 0.247, 0.307, 0.411, 0.373, 0.880	0.48	
16.03.23, 21.03.23	1000	0.528, 1.322, 1.234, 0.692, 0.948, 0.893, 0.853, 0.677	0.89	
DBCHexAO/ 13.02.23, 14.02.23	4000	0.0, 0.035, 0.004, 0.0, 0.0, 0.0, 0.003, 0.0	<0.01	
13.02.23, 16.02.23	2000	0.009, 0.056, 0.030, 0.016, 0.045, 0.026, 0.047, 0.034	0.03	
14.02.23, 16.02.23	1000	0.752, 0.419, 0.397, 0.474, 0.473, 0.421, 0.324, 0.722	0.49	Large plate crystals
DBCHepAO/ 09.03.23, 13.03.23	4000	0.008, 0.021, 0.005, 0.0, 0.0, 0.0, 0.014	<0.01	Small clear oil drops
13.03.23, 20.03.23	2000	0.061, 0.019, 0.011, 0.027,	0.02	Small clear oil drops

		0.008, 0.019, 0.029, 0.023		
13.03.23, 27.03.23	1000	0.219, 0.164, 0.324, 0.261, 0.447, 0.221, 0.211, 0.417	0.28	
DPCHexAO 25.04.23	4000	0.0, 0.015, 0.0, 0.004	<0.01	Cloudy solution
25.04.23	2000	0.005, 0.063, 0.004, 0.018	0.02	Cloudy solution
25.04.23	1000	0.815, 0.305	0.56	Cloudy solution
DPCHepAO 27.03.23, 28.03.23	4000	0.0, 0.006, 0.0, 0.0, 0.0, 0.0, 0.0, 0.0	<0.01	Small clear oil drops
03.04.23, 06.04.23	2000	0.167, 0.046, 0.133, 0.042, 0.046, 0.154	0.09	Small clear oil drops
04.04.23, 06.04.23	1000	0.997, 0.873, 0.705, 1.457, 1.355, 0.867	1.04	Small clear oil drops
DiPCHepAO 28.03.23, 30.03.23	4000	0.003, 0.0, 0.0, 0.0, 0.010, 0.0, 0.0	<0.01	Small clear oil drops
03.04.23, 11.04.23	2000	0.008, 0.242, 0.319, 0.122, 0.209, 0.214, 0.237, 0.132	------	Small clear oil drops, Plate crystals reached the beaker walls, so not reliable results.
04.04.23, 11.04.23	1000	1.699, 0.654, 1.207, 1.079, 0.449, 1.059, 0.782, 0.991	0.99	Small clear oil drops.

BDCPAO/ 09.02.23	4000	0.735, 1.563, 1.453, 1.501	1.30	Small yellow particles floating.
BDCHAO/ 18.04.23	4000	0.325, 0.404, 0.616, 0.341	0.42	Small clear oil drops.
18.04.23	2000	0.603, 1.705, 0.576, 0.778	0.91	Small clear oil drops
DBCHMAO/ 13.04.23	4000	0.049, 0.003, 0.007, 0.0, 0.022, 0.013	0.01	Small clear oil drops.
13.04.23, 14.04.23	2000	0.140, 0.089, 0.191, 0.109, 0.163, 0.078	0.12	Small clear oil drops.
13.04.23, 14.04.23	1000	0.551, 0.629, 0.893, 0.733, 0.727, 0.769	0.71	Small clear oil drops.

The 5-7 membered butylated cycloalkyl amine oxides DBCPAO, DBCHexAO, and DBCHepAO showed great crystal growth inhibition, whereas DBCHexAO and DBCHepAO showed the best inhibition properties with a result similar to TBAO even though the product did not dissolve completly. DBCHepAO showed a significantly better result on 1000 ppm than TBAO, with respectfully 0.28 g/h against 0.52 g/h. Figure 3.18 shows a graph with the visual representation of the average THF hydrate crystal growth rates for DBCPAO, DBCHexAO, DBCHepAO, TBAO, and TBAB at the following concentrations 4000 ppm, 2000 ppm, and 1000 ppm.

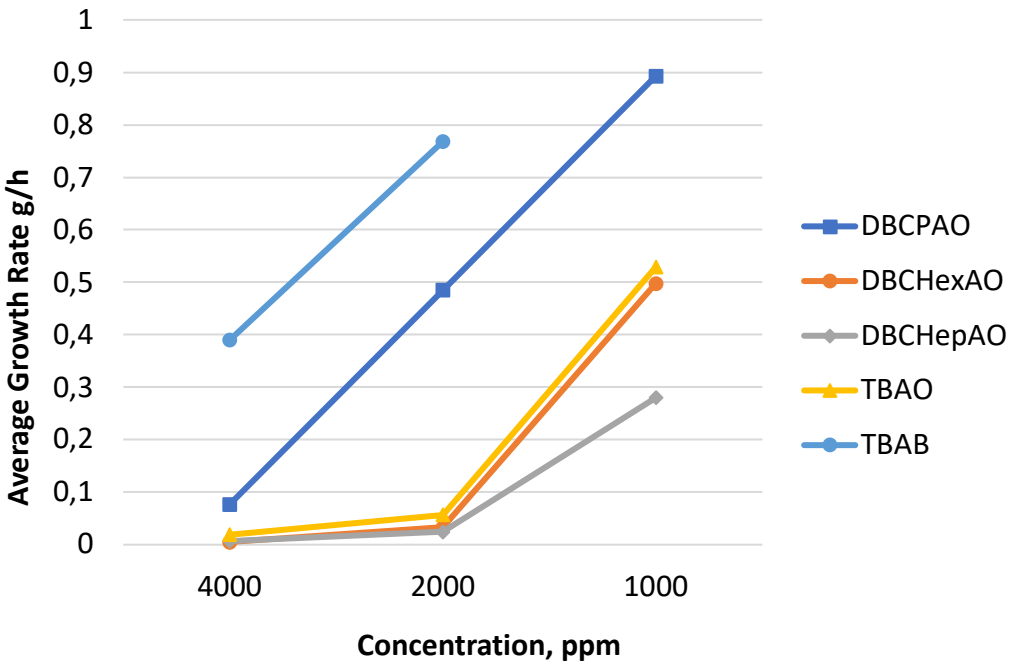

Figure 3.18 Average THF hydrate crystal growth rates for Di-n-butylcyclopentylamine oxide (DBCPAO), Di-n-butylcyclohexylamine oxide (DBCHexAO), Di-n-butylcycloheptylamine oxide (DBCHepAO), tri-n-butylamine oxide (TBAO), tetrabutylammonium bromide (TBAB) at several concentrations.

Since the 6- and 7-membered butylated cycloalkyl amine oxides worked the best at inhibiting THF hydrates, these were then alkylated with pentyl groups. DPCHexAO and DPCHepAO inhibited THF hydrates very well. Better than both TPAO and TPAB at the concentrations 4000 and 2000 ppm. At 1000 ppm, they both performed worse, which might indicate that the small undissolved oil droplets on top of the THF solution might have blocked the tip of the glass tube containing ice crystals at 4000 and 2000 ppm. This can result in the ice crystals not being in contact with the test solution, resulting in unreliable results. To ensure reliability, more tests, possibly with different equipment, on these two chemicals should be conducted. Figure 3.19 visually represents the average THF hydrate crystal growth rates for DPCHexAO, DPCHepAO, TPAO, and TPAB at several concentrations.

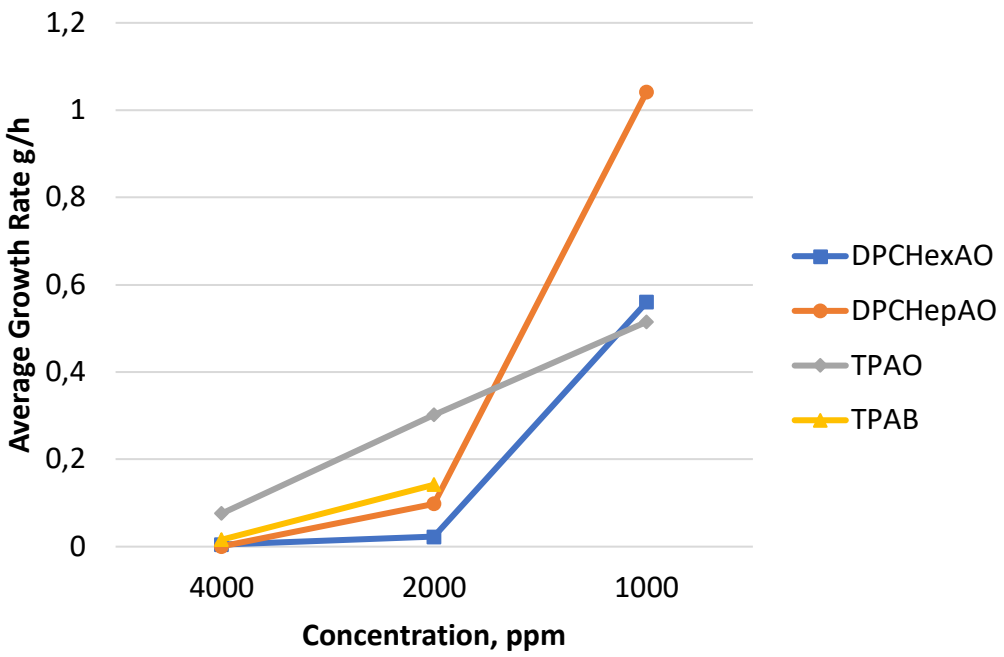

Figure 3.19 Average THF hydrate crystal growth rates for di-n-pentylcyclohexylamine oxide (DPCHexAO), Di-n-pentylcycloheptylamine oxide (DPCHepAO), tri-n-pentylamine oxide (TPAO), and Tetrapentylammonium bromide (TPAB) at several concentrations.

The 7-membered cycloalkyl amine oxide was then alkylated with iso-pentyl, as this ring size seemed to work the best at inhibiting THF hydrate. DiPCHepAO showed great inhibition with a <0.01 g/h growth with a concentration of 4000 ppm. This inhibition performance is the same as TiPAO and TPAB. At 2000 ppm, thin plate crystals were formed, touching the beaker walls, and the growth rate is then considered unreliable. The inhibition performance at 1000 ppm was considerably worse than the performance of TiPAO. This might again suggest that the small undissolved oil droplets blocked the tip of the glass tube and made the results unreliable. Figure 3.20 shows the THF crystal growth of DiPCHepAO at 1000 ppm.

Figure 3.20 THF hydrate crystal growth of Di-iso-pentylcycloheptylamine oxide (1000 ppm)

To see if the number of cycloalkyl groups attached to the amine would show a better or worse inhibition of THF hydrates, two compounds with two cycloalkyl structures, BDCPAO and BDCHAO, were synthesized. They both showed an inhibiting effect, whereas BDCHAO showed by far the best results of the two. Still, it did not have a better inhibiting effect than TBAB, so further tests were not continued. This might be because of steric impediments. We also wanted to see if the distance between the cycloalkyl group to the nitrogen atom in the amine showed a difference in the inhibition performance. We synthesized a butylated cyclohexyl group with one methyl group between the nitrogen and the cyclohexyl. DBCHMAO showed a good inhibiting performance but not as good as DBCHexAO, that does not have a methyl group. An alkylamine was butylated to confirm if the cycloalkyl group actually made a difference regarding the inhibition of THF hydrates. Di-n-butyl-4-heptylamine oxide showed a significantly worse performance at inhibiting THF hydrates with a growth of 0.23 g/h and 1.21 g/h at 4000 and 2000 ppm. As a comparison, the cycloalkyl amine oxide DBCHepAO had a crystal growth of <0.01 g/h and 0.02 g/h at the same concentrations. This confirms that a cycloalkyl group actually does matter regarding the inhibiting performance.

3.5.3 Amine Oxides with Heterocyclic Groups

Different amine oxides with heterocyclic groups have been synthesized and tested with the alkyl group n-butyl. This was carried out to determine if these chemicals could inhibit the hydrate crystal formation of THF hydrate. If they were successful further tests could be carried

out to see if they could potentially be used as both AAs and KHI synergists. Table 3.5 overviews the different heterocyclic amine oxides tested with simplified names. These are used later on in the discussion.

Table 3.5 Overview of the various heterocyclic amine oxides tested with simplified names.

Chemicals	Simplified name
N-butylpyrrolidine oxide	BPyrO
N-butylpiperidine oxide	BPipO
N-butylhexamethyleneimine oxide	BHMIO
1-butyl-4-methylpiperazine oxide	BMPipO
Di-n-butyltetrahydrofurfurylamine oxide	DBTHFFAO

The THF hydrate crystal growth rate results of the different amine oxides with heterocyclic groups at -0.3 °C on the THF rig can be seen in Table 3.6. The crystal growth is measured in grams/ hour.

Table 3.6 THF Hydrate Crystal Growth Rate (g/h) at -0.3 °C for Amine Oxides with Heterocyclic groups, measured for 1 hour at concentration 4000 ppm.

Chemical tested/ test date	Concentration (ppm)	Growth (gram/hour)	Average growth (gram/hour)	Comments
BPyrO/ 24.01.23, 26.01.23	4000	1.008, 1.782, 2.886, 3.001, 1.539, 2.724, 1.667, 2.125	2.09	A lot of crystal growth along the tubes.
BPipO/ 02.02.23	4000	0.894, 2.454, 1.443, 2.098	1.70	Whole crystal on the last three.
BHMIO/ 07.02.23	4000	2.019, 3.396, 2.064	2.40	One crystal fell into the beaker, so only three tests was reliable.
BMPipO 16.02.23, 20.02.23	4000	1.027, 1.259, 1.810, 1.529	1.40	

DBTHFFAO 20.02.23, 21.02.23	4000	0.112, 0.217, 0.153, 0.134, 0.173, 0.224, 0.177, 0.161	0.16

The 5-membered cycloimine BPyrO, the 6-membered cycloimine BPipO and the 7-membered cycloimine BHMIO showed very poor inhibition properties of THF hydrate with a result of 2.09 g/h, 1.70 g/h, and 2.40 g/h at 4000 ppm. Figure 3.21 shows the crystal growth of BPyrO at 4000 ppm on a glass tube. BPyrO and BHMIO promoted crystal growth since the result was 1.70 g/h without additives. We tried synthesizing di-n-butylaminopyrrolidine, but this compound was difficult to make, so we stopped synthesizing that chemical. The heterocyclic compound BMPipO had a minor inhibiting effect, with the result of 1.40 g/h, compared to the result without additives. However, this is still a very poor result. DBTHFFAO had a much higher inhibition than the rest of the heterocyclic amine oxides with 0.16 g/h at 4000 ppm. This is a better inhibition than the commercially used TBAB with 0.39 g/h at the same concentration. This might be due to the structure of the ring. The ring has the same five-sided cyclic ether structure as THF. However, the inhibition properties were not as good as several of the cycloalkyl amine oxides already discussed, so this compound was not tested further in this project. Still, it might be tested as a potential KHI synergist in future projects.

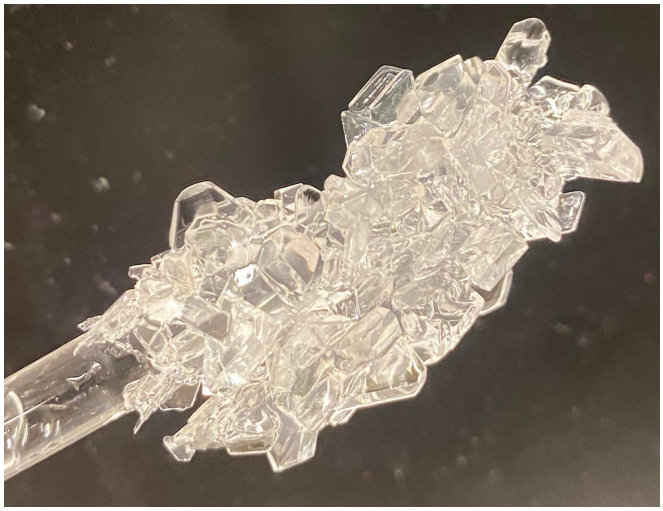

Figure 3.21 THF hydrate crystal growth of N-butylpyrrolidine oxide (4000 ppm).

3.6 References

(1) Kelland, M. A.; Kvæstad, A. H.; Astad, E. L. Tetrahydrofuran Hydrate Crystal Growth Inhibition by Trialkylamine Oxides and Synergism with the Gas Kinetic Hydrate Inhibitor Poly(N-Vinyl Caprolactam). *Energy Fuels* **2012**, *26* (7), 4454–4464. https://doi.org/10.1021/ef300624s.

(2) Zhang, Q.; Limmer, L.; Frey, H.; Kelland, M. A. *N* -Oxide Polyethers as Kinetic Hydrate Inhibitors: Side Chain Ring Size Makes the Difference. *Energy Fuels* **2021**, *35* (5), 4067–4074. https://doi.org/10.1021/acs.energyfuels.0c04333.

(3) Smith, M. B.; March, J. *March's Advanced Organic Chemistry: Reactions, Mechanisms, and Structure*; John Wiley & Sons, Incorporated: Somerset, UNITED STATES, 2013.

Chapter 4. Branched vs. Linear Polymers

The comparison between different VCap branched polymers' inhibition of THF hydrate crystal growth with the commercially used linear polymer Polyvinylcaprolactam (PVCap) will be covered in this chapter. This was measured by comparing the limiting concentration for zero growth (LCZG) on a THF rig.

4.1 Background

Polyvinylcaprolactam (PVCap) and other poly-N-vinyllactam polymers are commercially used KHIs in the oil and gas industry. The structure of PVCap can be seen in Figure 4.1. The polar part of the lactam ring, the amide group, forms hydrogen bonds with the water molecules located at the hydrate surface. In contrast, the non-polar part of the lactam ring gives van der Waals interactions where the small gas molecule would have entered the cage in the hydrate structure.[1, 2]

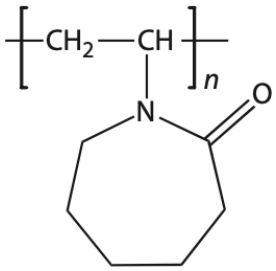

Figure 4.1 Polyvinylcaprolactam (PVCap).[3]

This project aimed to see if branched VCap polymers would inhibit THF hydrate growth better than the linear PVCap polymer. The limiting concentration for zero growth (LCZG) is measured when comparing the two. The crystals formed are usually thin, soft plate crystals that break off easily, making them impossible to measure accurately on a scale. The linear polymers used in this project were two different PVCap products, Luvicap EG and Luvicap EG HM. EG stands for Ethylene Glycol and is a THI. HM stands for High Molecular weight. The VCap branched polymers used in this project included trimethylolpropane triacrylate in isopropanol (iPrOH) with different lengths on its three branches (6:1 100% copolymer, 30:1, 60:1). Pentaerythritol tetraacrylate in iPrOH with different branched lengths (8:1, 20:1, 40:1, 80:1)

and the same polymer in butyl glycol ether (BGE) with a branched length of 20:1, both have 4 branches. Lastly, Bis pentaerythritol hexaacrylate with two branched lengths (8:1 100% copolymer, 40:1 in iPrOH). This polymer has 6 branches.

4.2 Results and Discussion

The THF hydrate crystal growth results of the different polymers at -0.3 °C on the THF rig can be seen in Table 4.1.

Table 4.1 THF Hydrate Crystal Growth test at -0.3 °C for Branched and Linear polymers.

Chemical tested/ test date	Concentration (ppm)	Growth	Comments
Luvicap EG / 30.01.23	4000	No growth	2 tests
30.01.23, 02.02.23	3000	No growth	4 tests
02.02.23	2000	Growth	2 tests, plates formed
02.02.23	2500	Growth	2 tests, no plates
06.02.23	2600	Growth	2 tests, no plates
06.02.23	2800	Growth	2 tests, no plates
06.02.23	2900	Growth	2 tests, no plates
Luvicap EG HM/ 18.04.23	2500	Growth	2 tests, plates formed
18.04.23	2000	Growth	2 tests, plates formed
20.04.23	3000	Growth	2 tests, no plates
20.04.23	3500	No growth	2 tests
25.04.23	3400	Growth	2 tests, no plates
Trimethylolpropane triacrylate (6:1)	3000	-----	Would not dissolve in THF/NaCl solution
Trimethylolpropane triacrylate in iPrOH (60:1)/ 07.02.23	3000	No growth	2 tests
07.02.23	2500	No growth	2 tests
07.02.23	2000	Growth	2 tests, almost no growth, no plates

09.02.23	2100	Growth	2 tests, no plates
Trimethylolpropane triacrylate in iPrOH (30:1)/ 20.02.23, 23.02.23	3000	Growth	4 tests, no plates
20.02.23, 23.02.23	3100	No growth	4 tests
Pentaerythritol tetraacrylate in iPrOH (8:1)/ 07.03.23	3000	Growth	1 test, no plates, but did not dissolve completely
23.03.23	3200	Growth	2 tests, no plates, but did not dissolve completely
	3500	-----	Would not dissolve in THF/NaCl solution
Pentaerythritol tetraacrylate in iPrOH (20:1)/ 07.03.23	3000	Growth	2 tests, no plates formed
23.03.23	3200	Growth	2 tests
14.04.23	3500	Growth	2 tests, did not dissolve completely
Pentaerythritol tetraacrylate in BGE (20:1)/ 06.03.23	3000	Growth	2 tests, did not dissolve completely, beakers full of crystal slush,
23.03.23	4000	Growth	2 tests, did not dissolve completely, plates formed
14.04.23	4500	Growth	2 tests, did not dissolve completely, plates formed
Pentaerythritol tetraacrylate in iPrOH (40:1)/ 14.04.23	3000	Growth	2 tests, no plates
14.04.23	3500	No growth	2 tests
15.04.23	3400	Growth	2 tests, no plates

Pentaerythriol tetraacrylate in iPrOH (80:1)/ 14.04.23	3000	Growth	2 tests, no plates
14.04.23	3500	No growth	2 tests
15.04.23	3400	Growth	2 tests, no plates
Bis pentaerythritol hexacrylate in iPrOH (8:1)/ 17.04.23	3000	Growth	2 tests, did not dissolve completely, no plates
18.04.23	4000	Growth	2 tests, did not dissolve completely, no plates
20.04.23	4500	No growth	2 tests, did not dissolve completely
Bis pentaerythritol hexacrylate (40:1)/ 17.04.23	3000	Growth	2 tests, did not dissolve completely, plates formed
18.04.23	4000	Growth	2 tests, did not dissolve completely, no plates
20.04.23	5000	Growth	2 tests, did not dissolve completely, no plates

The resulting LCZG for Luvicap EG was 3000 ppm, as expected, and Luvicap EG HM was 3500 ppm. According to previous studies, this result was unexpected as a higher molecular weight of PVCap should have had a better inhibition performance.[1] This might result from human error when measuring the concentration of the PVCap, or simply because the PVCap was not pure enough.

Before testing the branched VCap polymers on the THF rig, the solubility was tested in the THF solution. Many of the branched polymers were only partially soluble in the THF solution. Table 4.2 shows an overview of the resulting LCZG of the branched VCap polymers. Trimethylolpropane triacrylate (6:1) did not dissolve in the THF solution. This might be due to the short branches making the compound non-polar. Thus, no further tests were done.

Table 4.2 Overview of the resulting LCZG in ppm of the various VCap branched polymers.

VCap Branched Polymer	LCZG (ppm)
Trimethylolpropane triacrylate (6:1) 100% copolymer	-----
Trimethylolpropane triacrylate in iPrOH (60:1)	2100
Trimethylolpropane triacrylate in iPrOH (30:1)	3100
Pentaerythritol tetraacrylate in iPrOH (8:1)	>3500
Pentaerythritol tetraacrylate in iPrOH (20:1)	>3500
Pentaerythritol tetraacrylate in BGE (20:1)	>4500
Pentaerythritol tetraacrylate in iPrOH (40:1)	3500
Pentaerythritol tetraacrylate in iPrOH (80:1)	3500
Bis pentaerythritol hexacrylate in iPrOH (8:1)	4500
Bis pentaerythritol hexacrylate (40:1) 100% copolymer	>5000

Trimethylolpropane triacrylate (60:1) showed good inhibition of THF hydrates with an LCZG right above 2000 ppm. Not enough chemical was left to do a last confirmation test, but because there was very little growth on 2000 ppm, the assumed LCZG was set at 2100 ppm. This is better than both of the linear polymers and might be due to the similar length of the branches compared with the linear polymer chain on PVCap. Many of the branched VCap polymers got a worse solubility as the concentrations increased. This included the pentaerythritol tetraacrylate polymers with branch lengths of 8:1, 20:1, in iPrOH, and 20:1 in BGE. As mentioned above, this might be because of the short length of the branches resulting in non-polar compounds that are not water-soluble. The pentaerythritol tetraacrylate polymers with branch lengths of 40:1 and 80:1 resulted in an LCZG of 3500 ppm, the same as the Luvicap EG HM. The bis pentaerythritol hexacrylate polymers dissolved poorly in the THF solution and had an LCZG way above both PVCaps. Figure 4.1 visually represents the thin, soft crystal plates formed in a test beaker with the branched polymer (40:1) at 3000 ppm. Tests with synthetic natural gas mixtures might give different results as the conditions differ.

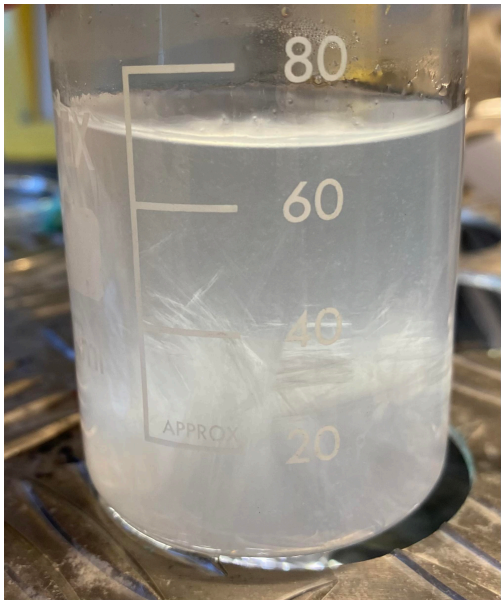

Figure 4.1 A beaker with THF hydrate plates from a test of 3000 ppm VCap: Bis pentaerythritol hexacrylate in iPrOH (40:1).

4.3 References

(1) O'Reilly, R.; Ieong, N. S.; Chua, P. C.; Kelland, M. A. Crystal Growth Inhibition of Tetrahydrofuran Hydrate with Poly(N-Vinyl Piperidone) and Other Poly(N-Vinyl Lactam) Homopolymers. *Chem. Eng. Sci.* **2011**, *66* (24), 6555–6560. https://doi.org/10.1016/j.ces.2011.09.010.

(2) Varma-Nair, M.; Costello, C. A.; Colle, K. S.; King, H. E. Thermal Analysis of Polymer–Water Interactions and Their Relation to Gas Hydrate Inhibition. *J. Appl. Polym. Sci.* **2007**, *103* (4), 2642–2653. https://doi.org/10.1002/app.25414.

(3) Kelland, M. A. *Production Chemicals for the Oil and Gas Industry*, 2nd ed.; CRC Press, 2014.

Chapter 5. Conclusion

In this first project, multiple amine oxides with different ring structures, cycloalkyl or heterocyclic, were synthesized and tested to see if they would inhibit THF hydrate crystal growth and have the potential to be used as both AAs and KHI synergists in the oil and gas industry. The cycloalkyl amine oxides showed excellent inhibiting performance of THF hydrates. Amine oxides with 6-7 membered cycloalkyl groups alkylated with butyl and pentyl showed an excellent inhibition performance. They inhibited THF hydrates better than TBAB, TPAB, TBAO, and TPAO at certain concentrations and should be further tested on gas hydrates as KHI synergists or AAs. Amine oxides with two cycloalkyl groups had poor inhibiting performance compared with cycloalkyl amine oxides with one ring structure. It was confirmed that an amine oxide with one cycloalkyl group actually does matter regarding the inhibiting performance. An alkylamine was butylated to compare. The heterocyclic amine oxides gave poor inhibiting performances of THF hydrate with a concentration of 4000 ppm. The tests on these compounds were therefore ended. Di-n-butyltetrahydrofurfurylamine oxide (DBTHFFAO) was one exception. This organic compound gave a better inhibition performance than the commercially used TBAB. DBTHFFAO should be further tested as a KHI synergist and a possible AA in future projects.

The thesis's second project entailed comparing the inhibition of THF hydrates with the commercially used linear polymer PVCap and different already synthesized VCap branched polymers. Most of the branched VCap polymers were not water-soluble enough to be dissolved completely and needed a much higher LCZG than the linear polymers. Thus, many compound tests ended before the LCZG was confirmed. Only one branched polymer got a lower LCZG than Luvicap EG (3000 ppm), the trimethylolpropane triacrylate polymer with three branches (60:1) with an LCZG of 2100 ppm.

Appendices

Di-n-butyl-4-heptylamine in $CDCl_3$ (400MHz ^{1}H-NMR)

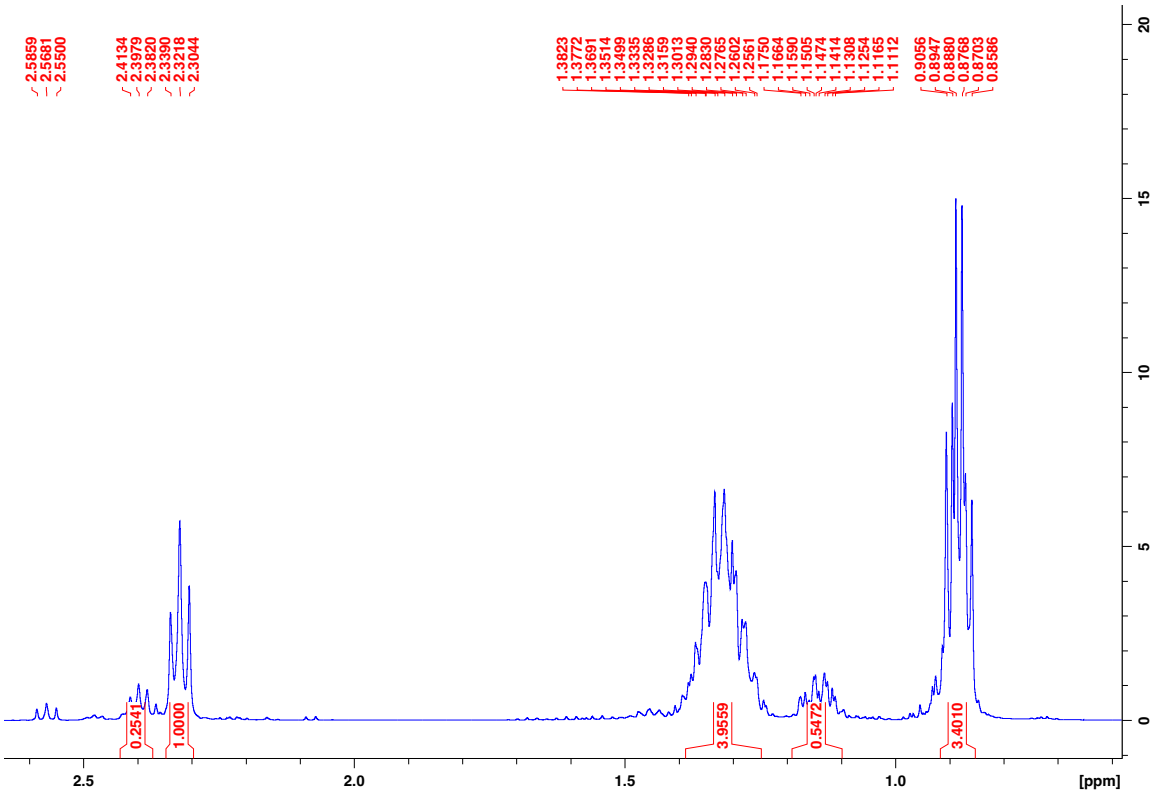

Di-n-butylcyclopentylamine in $CDCl_3$ (400MHz ^{1}H-NMR)

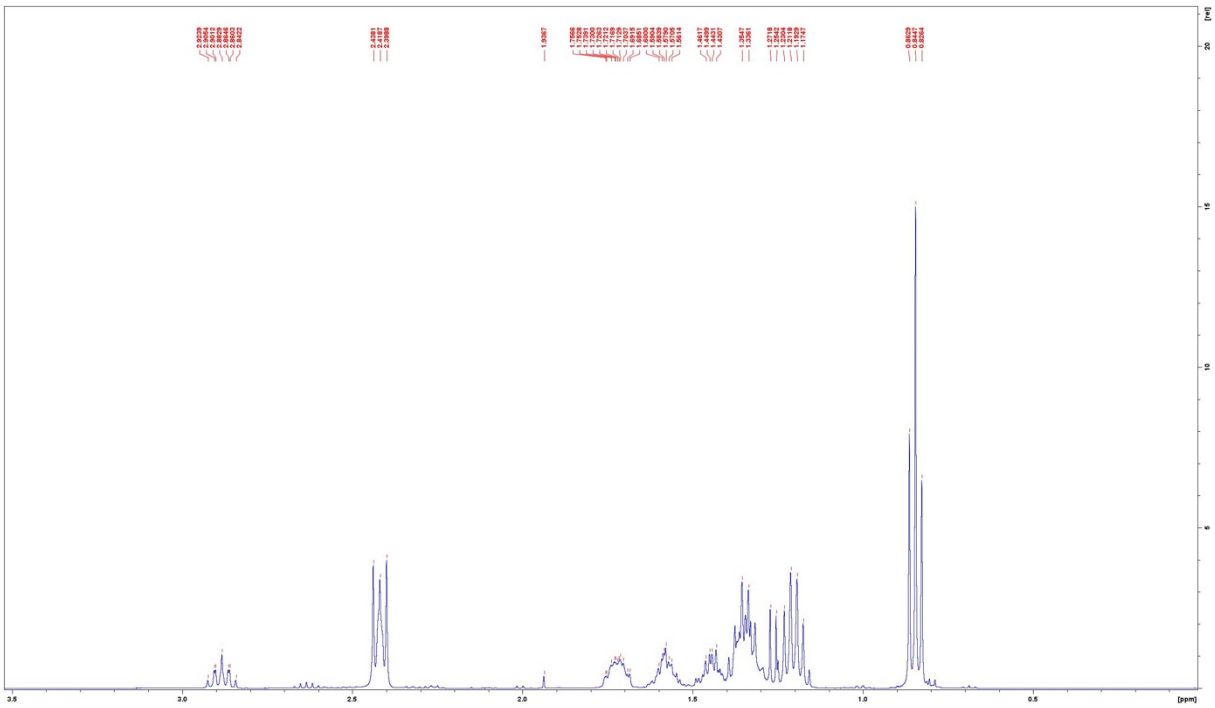

Di-n-butylcyclohexylamine in $CDCl_3$ (400MHz ^{1}H-NMR)

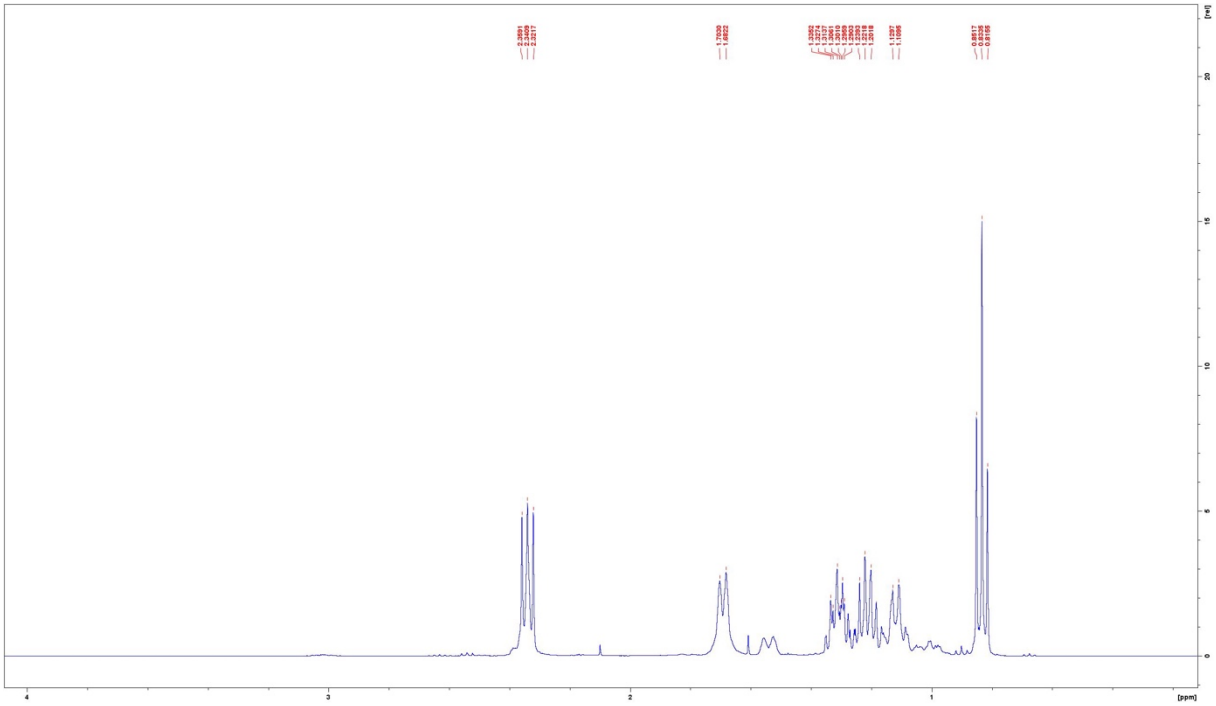

Di-n-butylcycloheptylamine in $CDCl_3$ (400MHz ^{1}H-NMR)

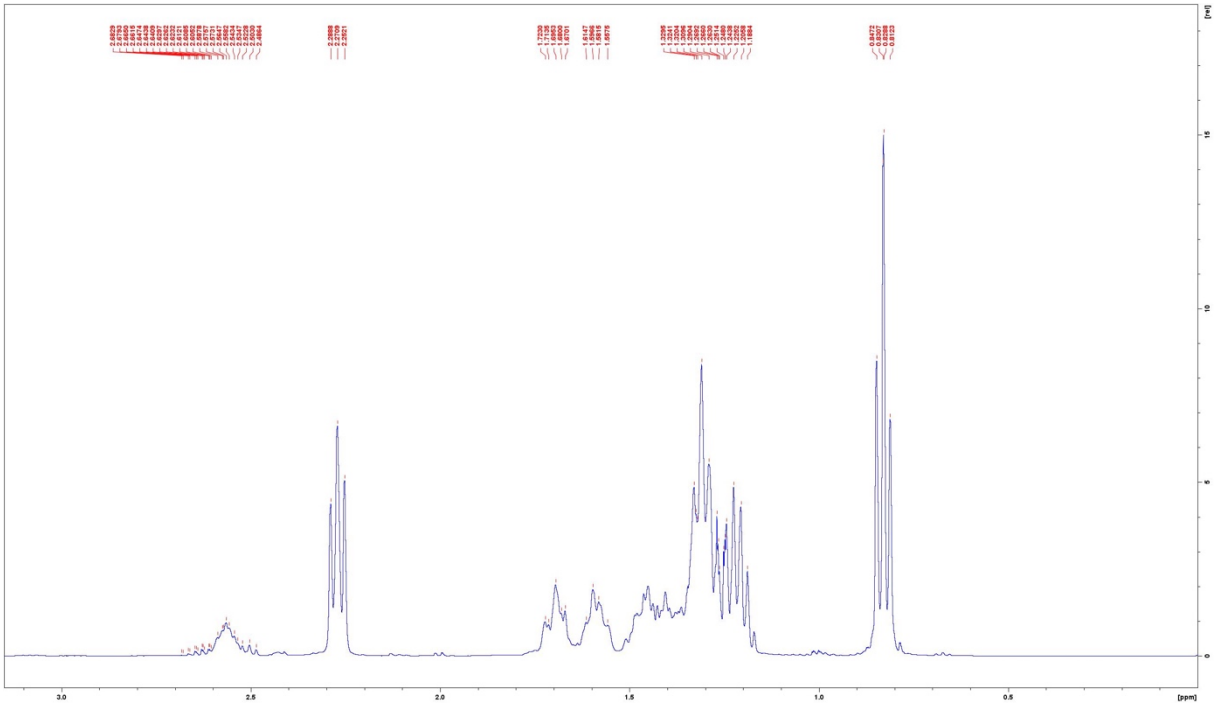

Di-n-pentylcyclohexylamine in $CDCl_3$ (400MHz ^{1}H-NMR)

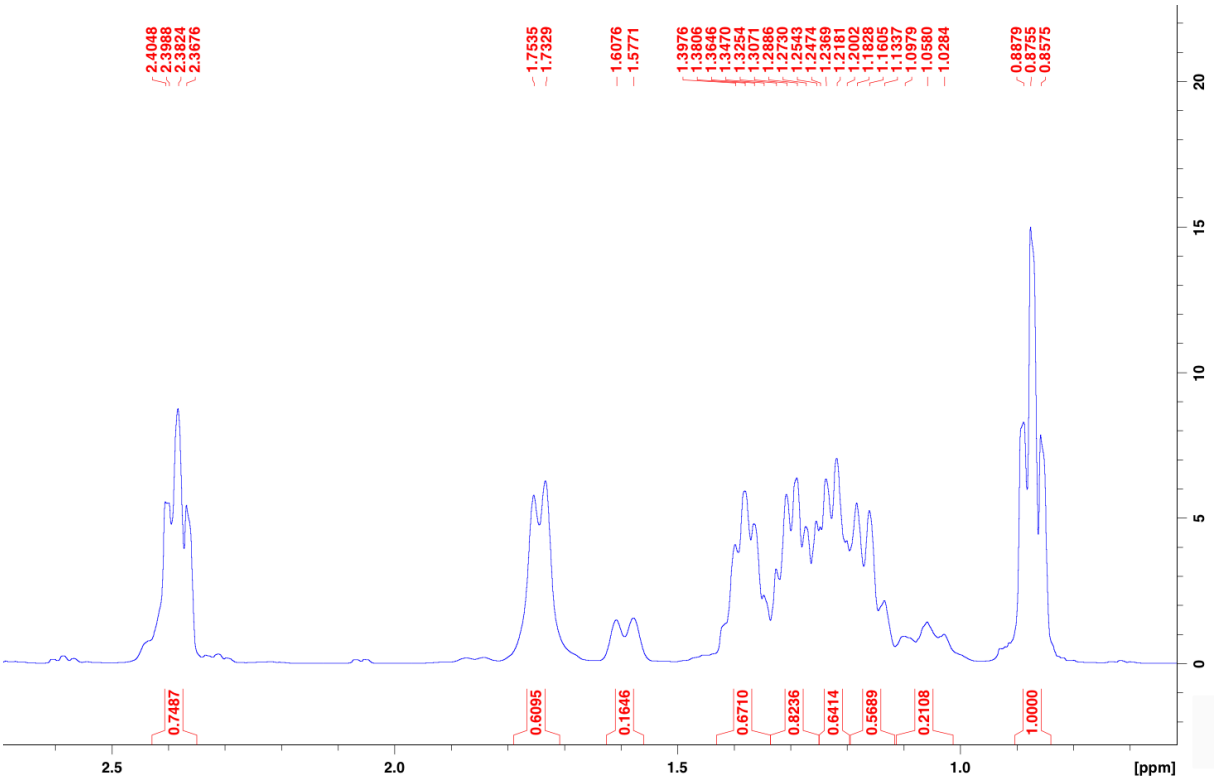

Di-n-pentylcycloheptylamine in $CDCl_3$ (400MHz ^{1}H-NMR)

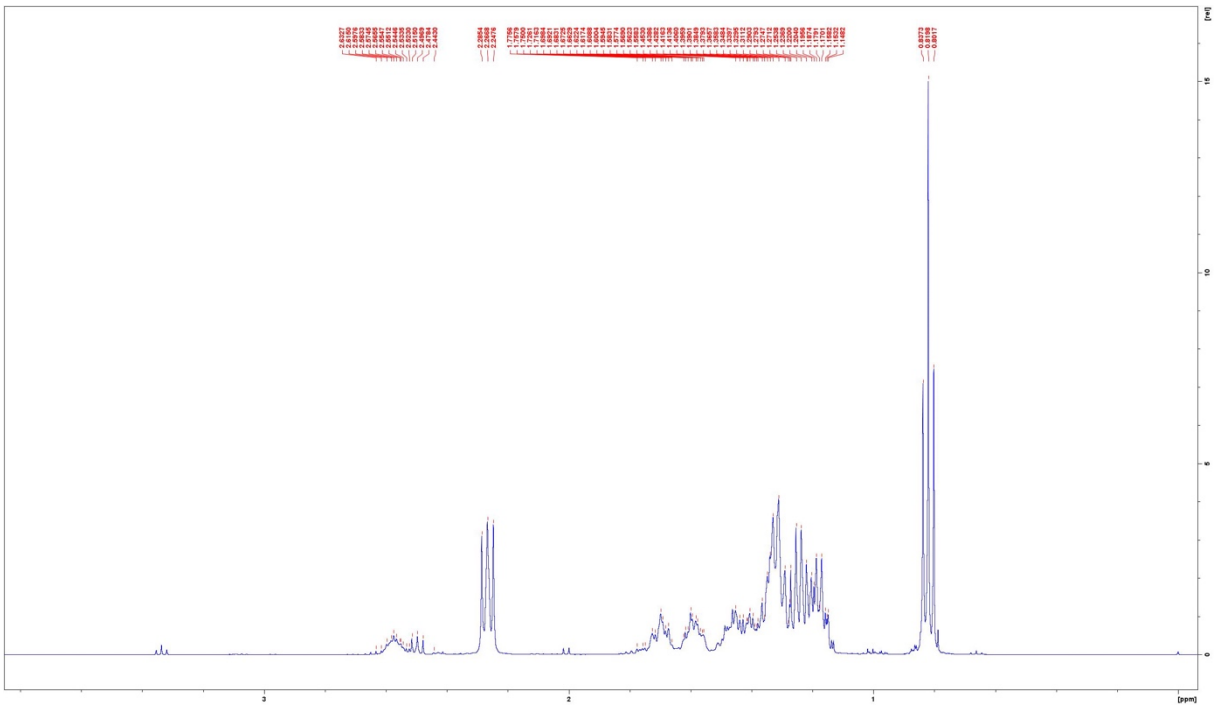

Di-iso-pentylcycloheptylamine in $CDCl_3$ (400MHz ^{1}H-NMR)

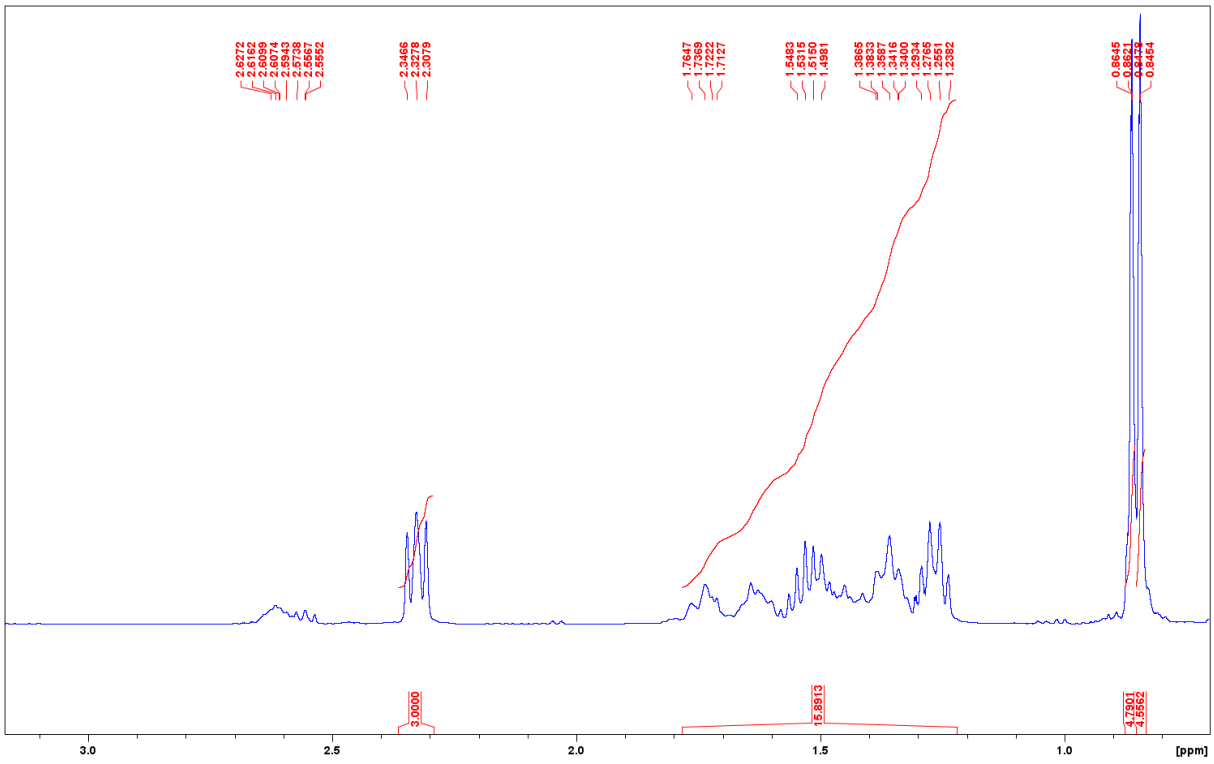

N-butyldicyclopentylamine in $CDCl_3$ (400MHz ^{1}H-NMR)

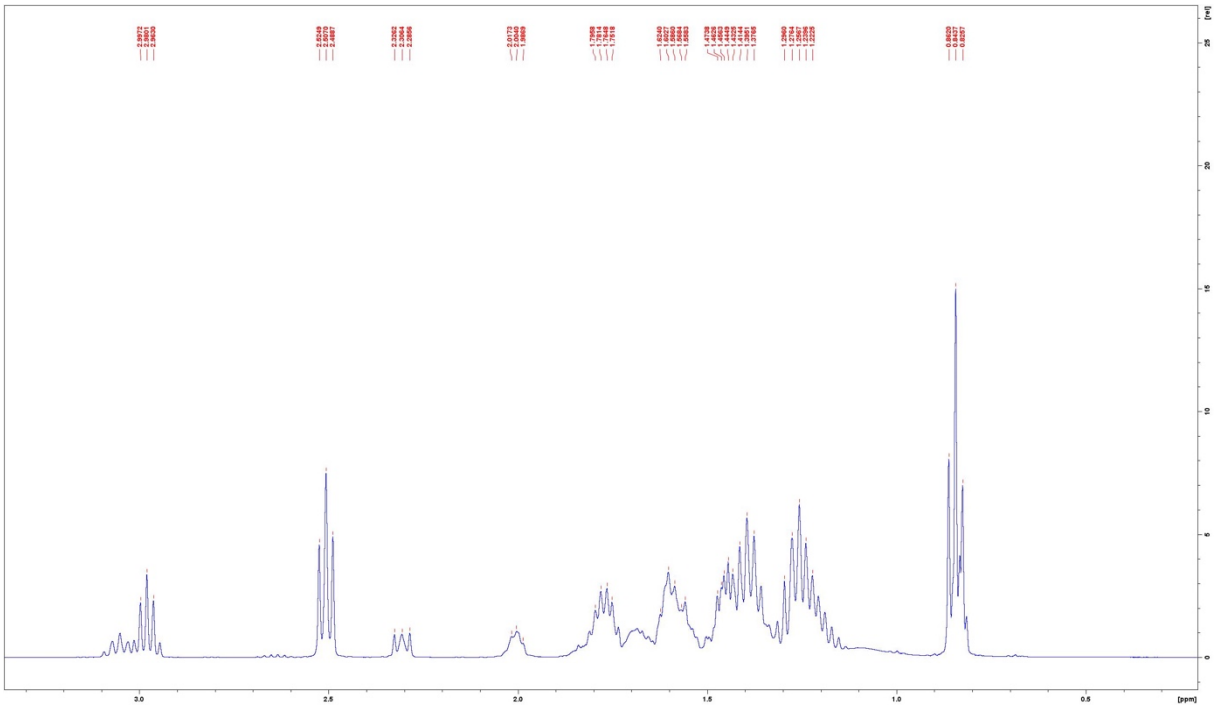

N-butyldicyclohexylamine in $CDCl_3$ (400MHz ^{1}H-NMR)

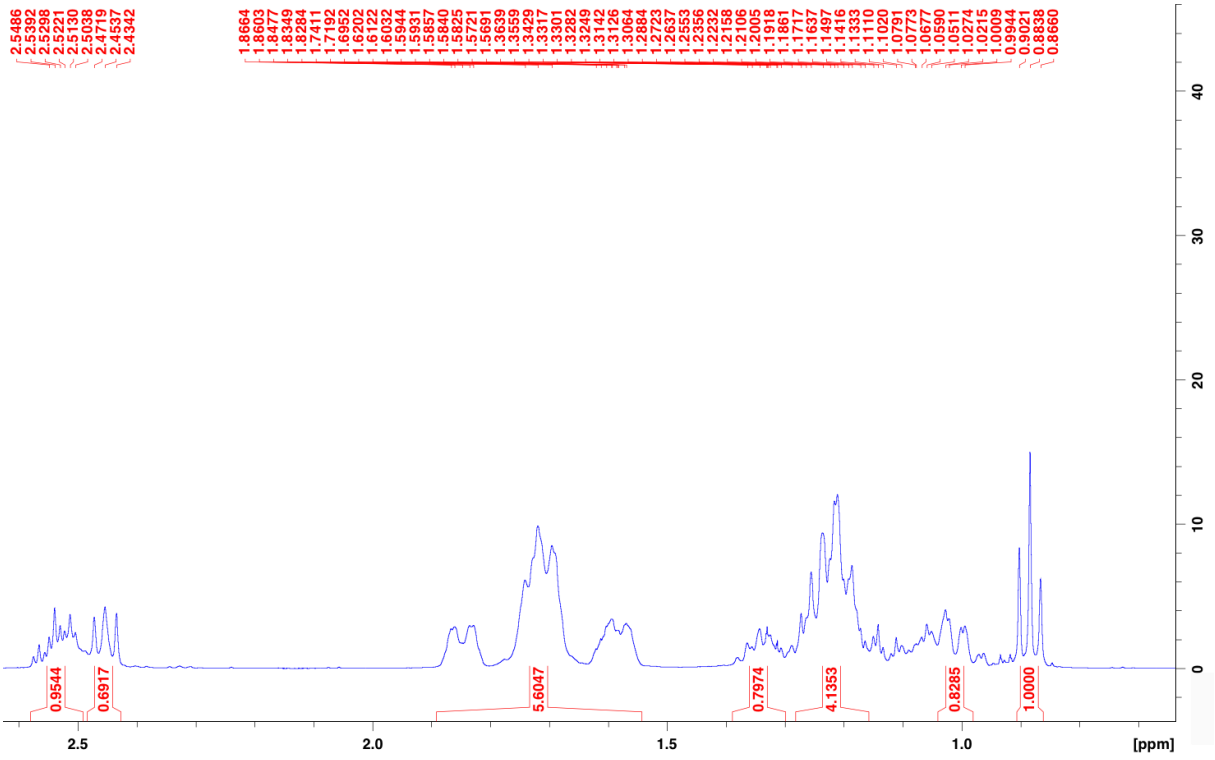

Di-n-butylcyclohexanemethylamine in $CDCl_3$ (400MHz ^{1}H-NMR)

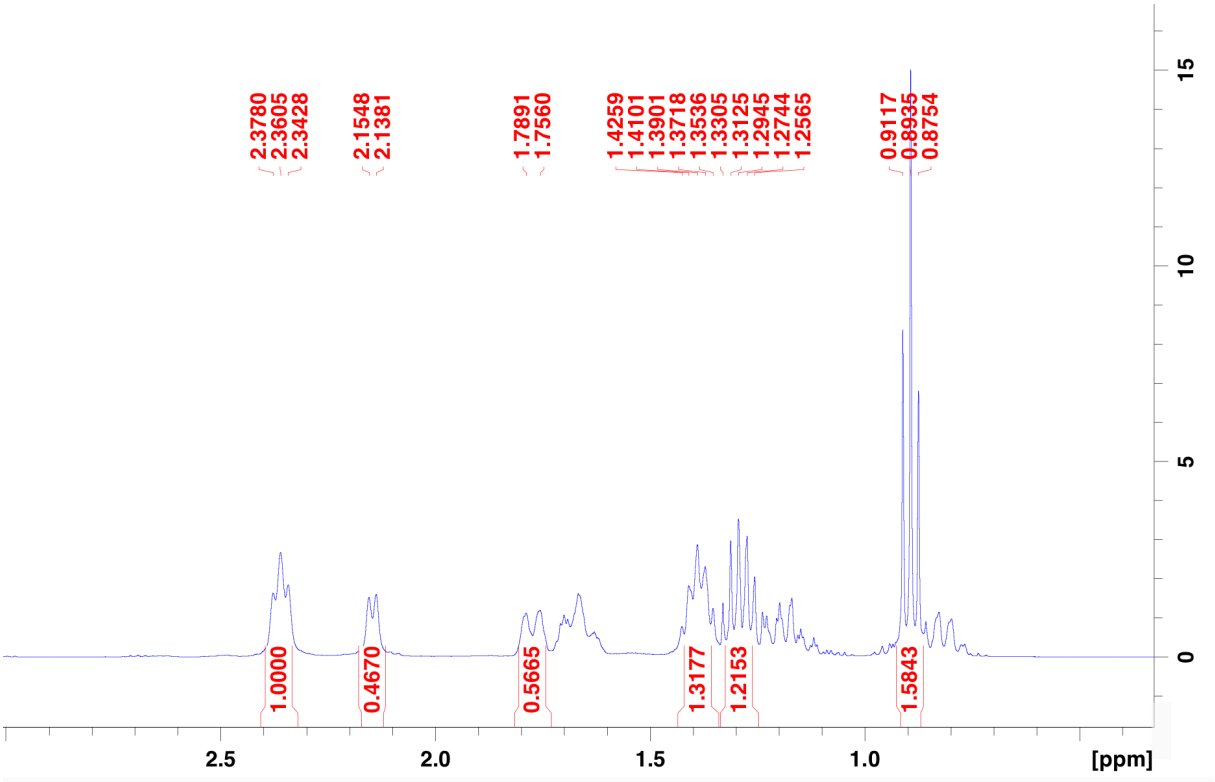

N-butylpyrrolidine in $CDCl_3$ (400MHz ^{1}H-NMR)

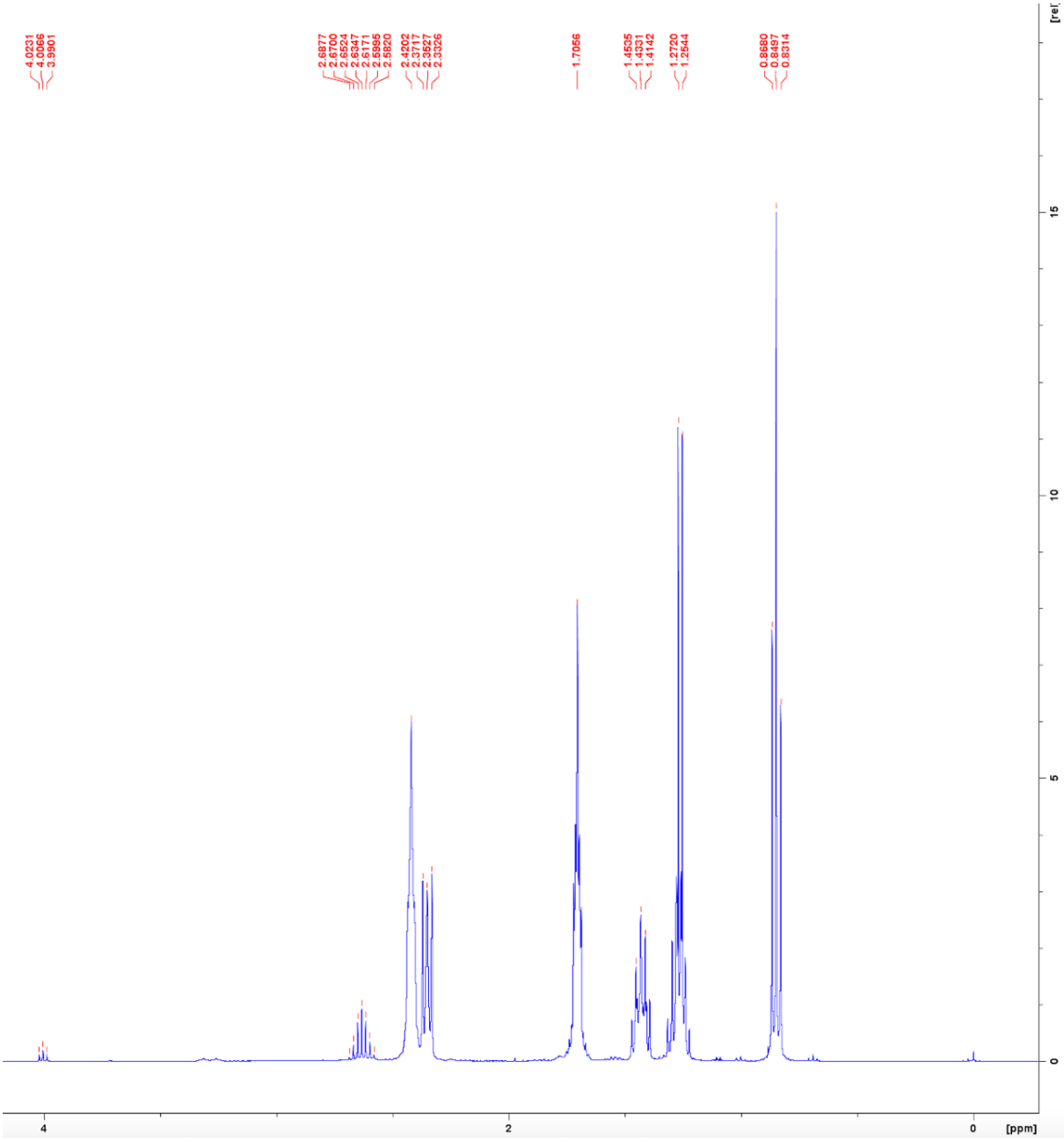

N-butylpiperidine in $CDCl_3$ (400MHz ^{1}H-NMR)

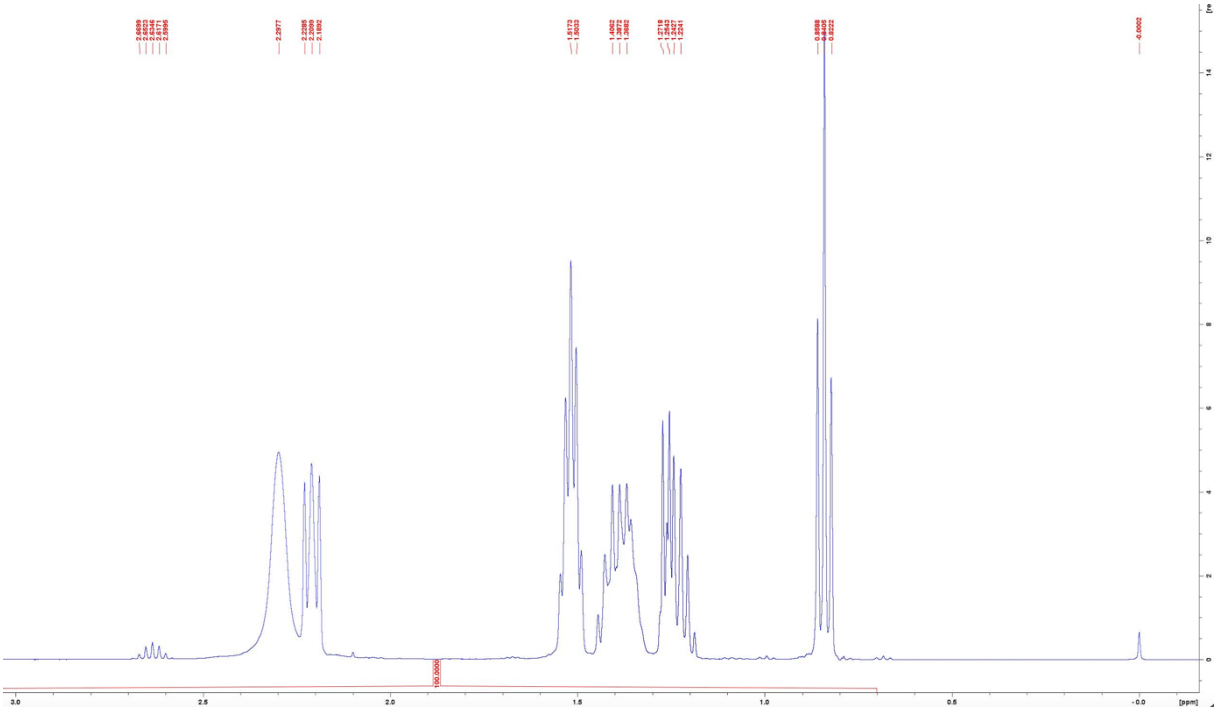

N-butylhexamethyleneimine in $CDCl_3$ (400MHz ^{1}H-NMR)

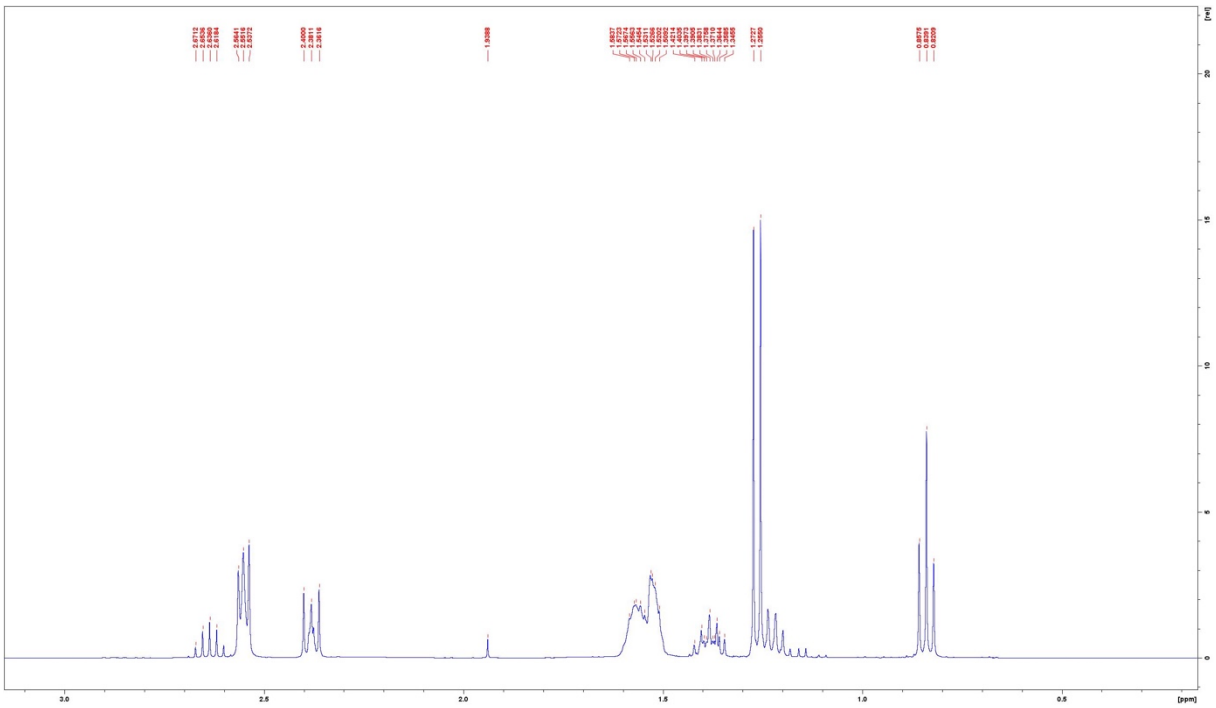

Di-n-butylaminopyrrolidine in $CDCl_3$ (400MHz ^{1}H-NMR)

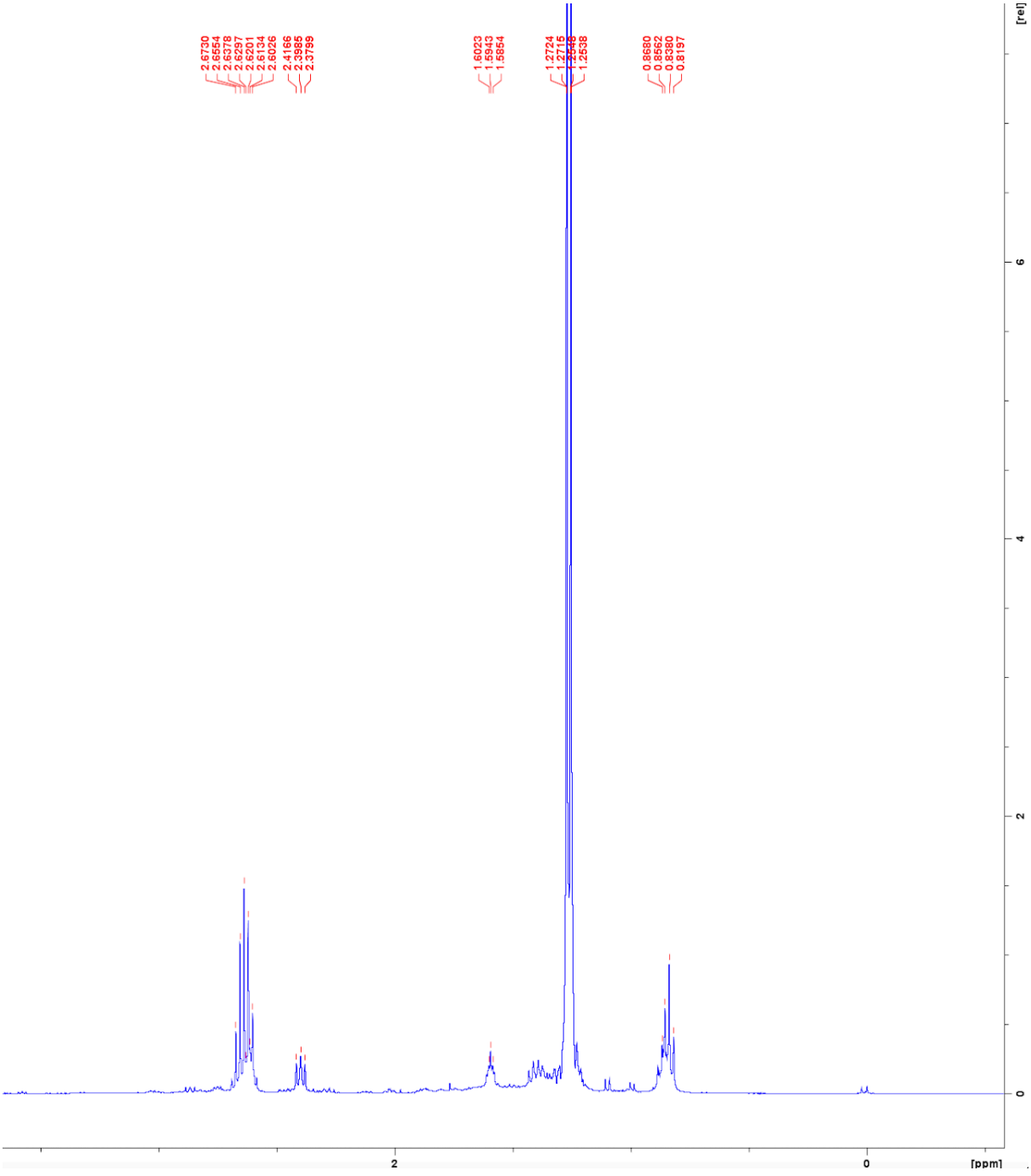

1-butyl-4-methylpiperazine in $CDCl_3$ (400MHz ^{1}H-NMR)

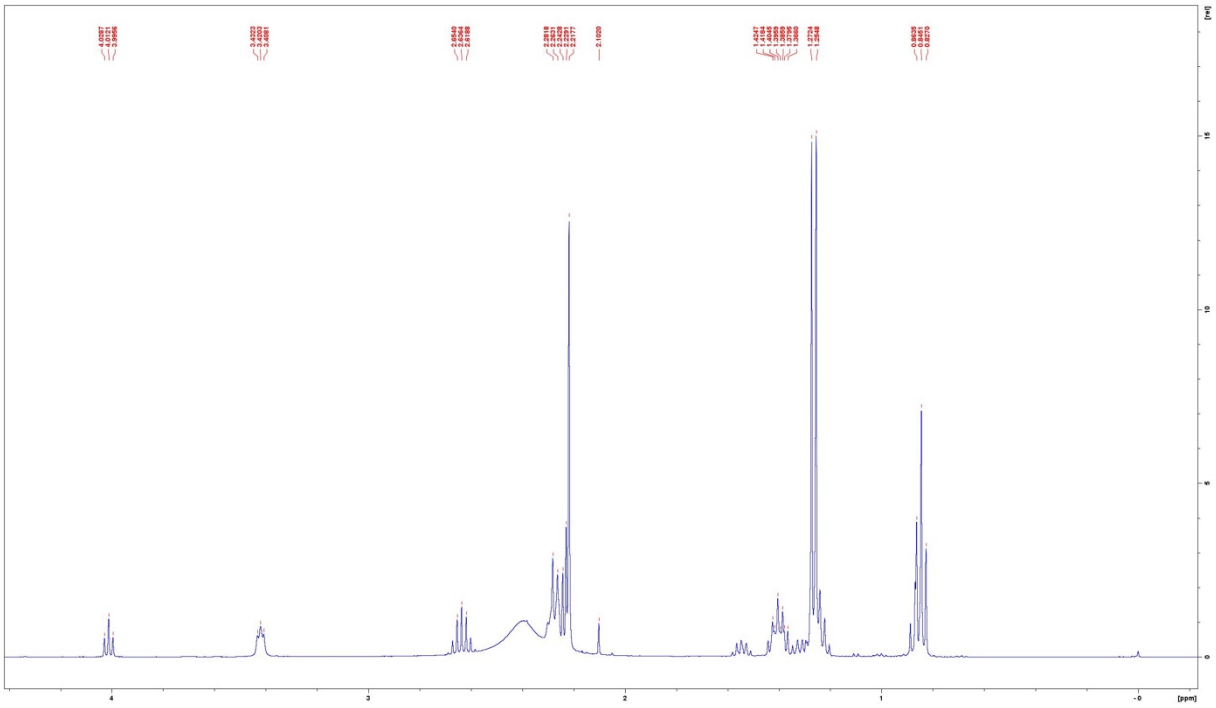

Di-n-butyltetrahydrofurfurylamine in $CDCl_3$ (400MHz ^{1}H-NMR)